BIOMIMETIC BOUNDARY LUBRICANTS TO BIND TO AND PROTECT CARTILAGE

A Dissertation Presented to the Faculty of the Graduate School of

Cornell University

In Partial fulfillment of the Requirements for the Degree of

Doctor of Philosophy

by

Kirk Jerome Samaroo

August 2015

BIOMIMETIC BOUNDARY LUBRICANS TO BIND TO AND PROTECT CARTILAGE

Kirk Samaroo, Ph.D.

Cornell University, 2015

The glycoprotein lubricin is the primary boundary lubricant of articular cartilage. In injured joints, supplementation with lubricin prevents further damage. The lubricating and chrondroprotective abilities are believed to be linked. Furthermore, the lubricating abilities of lubricin are thought to arise from its structures. The C-terminus of lubricin binds the molecule to an articulating surface, and the hydrophilic oligosaccharide brush draws and traps water near the surface. These structures work in tandem to hydrate articulating surfaces, imparting lubrication and facilitating movement.

Since this boundary lubricating mechanism is thought to arise from lubricin's structure, a series of poly(acryilic acid)-*graft*-polyethylene glycol (pAA-*g*-PEG) brush co-polymers were synthesized. The copolymers were equipped with a thiol terminus to bind them to surfaces much like the C-terminus of lubricin. By mimicking the hydrophilic, brush-like structure of lubricin, pAA-*g*-PEG copolymers were effective boundary lubricants of articular cartilage. Using different pAA backbone sizes and PEG side chain sizes, the lubricin-mimetics were tuned to create surfaces of different characteristics and different lubricating abilities. To tune their lubricating domain, pAA-*g*-PEG polymers were bound to gold surfaces by self-assembly via a terminal thiol.

The pAA-*g*-PEG copolymers then effectively mimicked the structure and function of the cartilage lubricant lubricin. A library of eight polymers were synthesized with varying pAA

backbone size, PEG side chain size, and PEG:AA side chain density. They bound to cartilage surfaces with binding time constants ranging from 20 to 41 min, and polymer binding was proportional to their lubricating ability. Six of the eight lubricin-mimetics effectively lubricated cartilage surfaces in vitro, with two mimetics lubricating more effectively than the lubricin-mutant LUB:1.

This work provides evidence supporting approaches to mitigate cartilage damage using boundary lubricants. The lubricin-mimetics created in this study mimic only lubricin's structure, yet demonstrated the ability to both lubricate and protect cartilage. This ability was manipulated by varying the size of the components of the mimetics, and more effective lubricants resulted in better preservation of the cartilage tissue in injured joints evident by both the preservation of the cartilage's lubricating surface and histologic OARSI scoring. Thus, lubricants that lubricate cartilage more effectively when administered in vitro can be used as a screening process to determine the lubricant's effectiveness at protecting cartilage in vivo and preventing injury and disease progression.

BIOGRAPHICAL SKETCH

Kirk Samaroo was born on the island of Trinidad in the southern Caribbean Sea. At the age of five, he travelled with his parents as they moved to the USA in search of better opportunities. He later received a Bachelor of Science in each of the fields of Mechanical Engineering and Mathematics from the Massachusetts Institute of Technology. He has since started his PhD studies at the Sibley School of Mechanical and Aerospace Engineering at Cornell University under the guidance of Dr. Lawrence Bonassar.

To my parents: Cyril and Ousha Samaroo

ACKNOWLEDGMENTS

I would like to thank my parents first and foremost. To them, I owe my life. Without their support and encouragement, this work would not have been possible. Also, my gratitude goes out to my brother Kevin and his wife Anna for putting up with me for all of these years.

Thank you to my academic advisor, Lawrence Bonassar, Ph.D. I had dreams of studying microfluidic systems when starting graduate school at Cornell, but Larry made a compelling case for the fulfillment and meaning that I ended up finding in biomechanics and tissue engineering.

My thanks also extend to my primary collaborators Dr. David Putnam and Dr. Mingchee Tan, without whom this project would have been literally impossible to accomplish. I would also like to thank all of my collaborators and advisors on this project: Dr. Poul Petersen, Dr. Delphine Gourdon, Dr. Roberto Andresen-Eguiluz, Dr. Scott Rodeo, Ashley Titan, and Camila Carballo, Sarah Forcier, and Aliyah Barrett.

My gratitude to my funding sources: the Sage Fellowship, the Provost Diversity Fellowship, the NIH, CCMR, CAT, and NYSTAR. And a special thanks goes to the Bonassar Laboratory. We have been through a variety of highs and lows, and I have had their support through them all.

TABLE OF CONTENTS

TABLE OF FIGURES

TABLE OF TABLES

1.0 Introduction

1.1 Articular Cartilage

1.1.1 Structure and function. Articular cartilage is the smooth tissue that coats the articulating ends of bones in joints. The primary physiological function of cartilage is to provide a low friction interface that distributes loads across joints.[1] Even with relatively low cell density, a dense extracellular matrix, and limited vascularization, cartilage was designed to provide this function over millions of cycles per year and a lifetime of use. The tissue is comprised of approximately 75% water, 5% chondrocytes and 20% a complex heterogeneous extracellular matrix (ECM).[2] The ECM consists of mostly proteoglycans and collagen, with aggrecan and type II collagen being the most prevalent of the molecules by dry weight, respectively.[3] (Figure 1.1)

Articular cartilage is a stratified tissue that can be described in zones, most notably a superficial, and deep zones each having unique properties. These zones are bookended by the articular surface and a calcified region where the cartilage integrates with subchondral bone. Proteoglycans and collagen form the primary architecture of cartilage. Type II collagen covalently links to type IX collagen forming a collagen network throughout the stratified tissue[4]; the orientation of the collagen fibers differ within each zone. Protoeglycans consist of sulfated glycosaminoglycans (GAG) bonded to a large core protein.[5] The interaction between the charged proteoglycans, the collagen network, and the surrounding fluid provides cartilage with its bulk material properties. The tensile and shear properties are dominated by solid ECM components, most notably the collagen network, and are largely independent of fluid flow effects.[6]

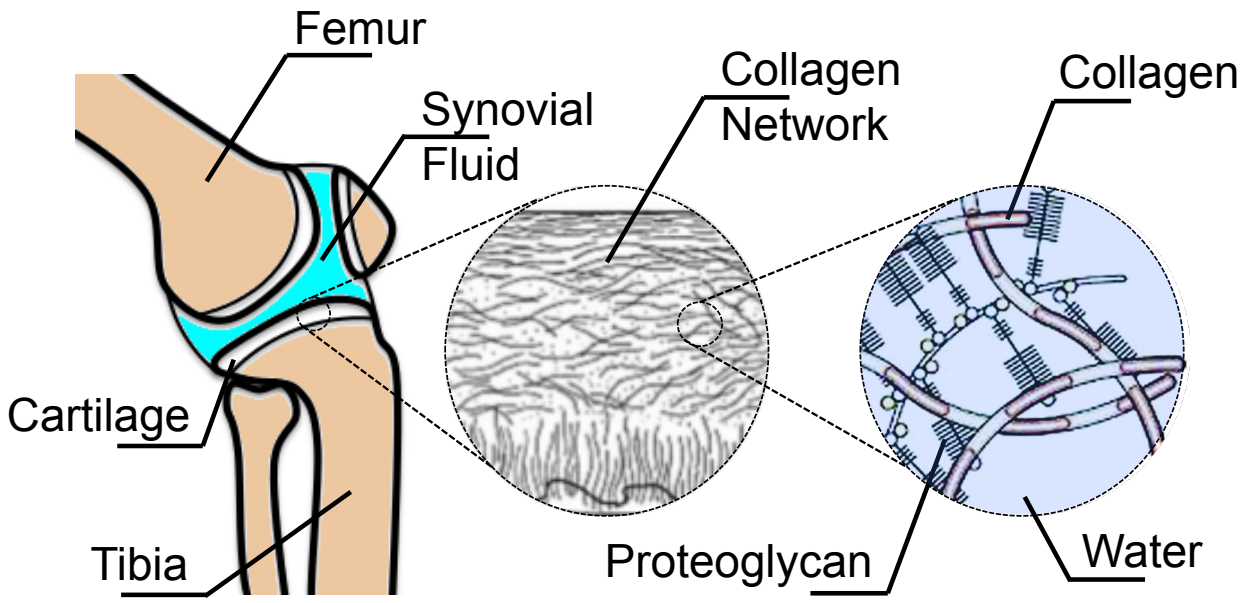

Figure 1.1. Schematics of a typical knee joint is shown with the macro- and microstructure of cartilage.

The compressive[7] and frictional properties[8] of articular cartilage are governed by the interplay of its three major components. Compression of the tissue results in the pressurization of the interstitial fluid within the ECM. As the fluid is exuded from the tissue, the pressure dissipates. During this time, the load support of the system transitions from the fluid to the matrix. After the interstitial fluid equilibrates, the compressive behavior of the tissue is largely governed by electrostatic repulsions between neighboring GAG chains[9], which reduce the compaction of the tissue. If the compressive load is subsequently reduced, the charged GAGs rehydrate the tissue through osmotic pressure[10], with osmotic swelling curbed by the collagen network[2].

The orientation of collagen fibers and the hydrated GAGs largely explain the mechanisms describing the distribution of loads across the joint, but another primary function of cartilage is to provide a low friction bearing surface. The time-dependent, biphasic compressive properties of cartilage directly contribute to its biphasic frictional behavior.[8,11,12] Fluid pressurization creates fluid flow throughout the tissue, which in turn results in a low initial friction coefficient. As the fluid dissipates and supports less of the normal load, the lubrication of the cartilage depends more on the constituents of the articular surface and friction coefficients rise monotonically until the fluid pressure equilibrates and an equilibrium friction coefficient is reached.

1.1.2 Injury and disease. At the relatively high equilibrium friction coefficients, the frictional properties of cartilage depend more on the ECM components located at the articular surface. And due to its limited capacity for self-repair, diseased or damaged cartilage surfaces have higher friction coefficients which leads to more wear and more damage[13], as is the case with osteoarthritis (OA).

OA is a degenerative disease characterized by the degradation of cartilage and other tissues in joints.[14] The disease progression leads to fissures in the cartilage surface, collagen fibrillation, and loss of tissue.[15] These changes can occur due to biological changes with age[16,17] or through traumatic injury[18]. The result is a painful and debilitating disease that limits mobility and reduces quality of life. Continued use of diseased joints causes further cartilage degradation and erosion, suggesting that mechanical phenomena contribute strongly to the degradative process.

OA is the leading cause of disability in the US affecting more than 27 million adults in 2003[19], a number projected to climb to 67 million by 2030 as the population ages and obesity rates rise[20]. One in two people will develop OA within their lifetime, two in every three in the obese population. It is a widespread disease for which medical science does not have a cure or viable treatment to inhibit progression of the disease.

Current pharmacologic treatments of OA are aimed at symptom relief. Primarily, pain management and anti-inflammatories, such as non-steroidal anti-inflammatories[21] and intra-articular corticosteroid injections[22], temporarily restore function to diseased joints but have little to no effect on disease progression. Other treatments include nutritional supplements such as chondroitin sulfate or glucosamine supplements[23], which are supposed to stimulate regrowth and restoration of the joints, but there is little evidence in the medical or academic communities exists to support that claim.

A more recent approach to the treatment of OA involves the use of injectable lubricants to minimize friction and tissue damage. A common approach involves the intra-articular injection of the natural synovial glycosaminoglycan, hyaluronic acid (HA)[24], also known as HA viscosupplementation. HA is a nonsulfated GAG that is naturally found in synovial fluid and cartilage, and is an effective lubricant of cartilage.[25] HA viscosupplementation was originally

approved by the FDA claiming injections alleviated pain in mild to moderate cases of OA, but the idea behind HA viscosupplementation is to add a lubricant to diseased or injured joints to prevent wear and further degradation of joint tissue. However, the efficacy of HA injections are a topic of continued debate, with studies showing only transient effects on pain relief[26] that are minimally better than placebo[27] and inconsistent evidence of benefit in radiographic assessment of disease progression[28]. The mechanisms of joint lubrication can provide an explanation for the minimal efficacy of HA treatments.

1.2 Tribology

Classical tribology can be used to explain key mechanisms of joint lubrication. Tribology is the study of how surfaces in relative motion interact, and involves friction, lubrication, and wear. Friction is defined as a force that acts in opposition to the motion of the surfaces, and is governed by their relative interaction. Most commonly, friction is quantitatively measured and reported through a friction coefficient μ, a dimensionless ratio between the tangential friction force and the normal force, $\mu = {F_{\parallel}}/{F_{\perp}}$. The coefficient of friction is not simply a material property, but instead is a relationship between the two interacting surfaces that depends on the materials, fluid medium, and operating conditions.

1.2.1 The modes of lubrication. To better understand the relationship between two opposing articulating surfaces, the Stribeck curve (Figure 1.2) relates the coefficient of friction against the Hersey[29] or Sommerfeld[30] numbers to display three distinct modes of lubrication: boundary, mixed, and fluid lubrication. The Hersey and Sommerfeld numbers are dimensionless parameters that depend on the relative articulating velocity of the surfaces, fluid dynamic viscosity, the

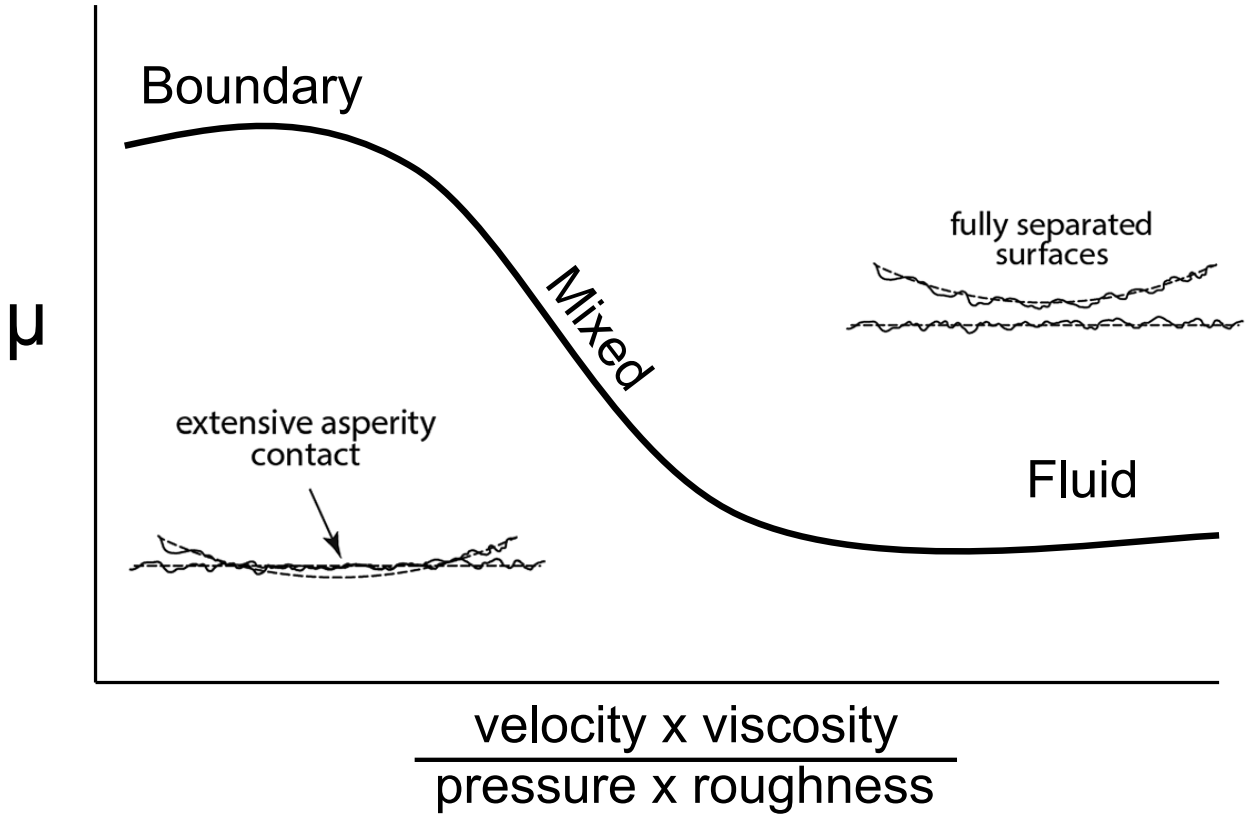

Figure 1.2. This Stribeck curve shows how friction changes with the parameters velocity, viscosity, pressure, and surface roughness. Fluid plays a larger role in friction as the Sommerfeld number increases.

normal pressure, and a characteristic length such as rotational bearing radius (Hersey), effective surface roughness, bearing clearance, or contact length (Sommerfeld)[30–33].

Fluid lubrication is so named because within this mode the friction load is supported mostly by the bulk fluid. Furthermore, the frictional properties of two surfaces in motion primarily depend on the material properties of the bulk fluid, specifically the fluid viscosity.[34] This regime can be broken down further and could include or may be referred to as fluid film, hydrodynamic, or elasto-hydrodynamic lubrication among others. For classical materials in fluid lubrication, the separation distance between opposing materials is greater than that of the mean surface roughness leading to the formation of fluid film.[34,35] While soft and porous materials might not develop full fluid films as easily, the fluid load support and bulk fluid properties play a similar role in influencing frictional behavior in fluid lubrication.[33,36,37]

By contrast, frictional properties of boundary lubrication are primarily governed by solid-solid interactions. Within this mode, the opposing surfaces are in significant solid-solid contact, and the mean separation distance is less than that of their average surface roughness. In boundary lubrication, friction coefficients are greatest resulting in the highest frictional forces and most wear. As a result, the friction and wear between materials in boundary lubrication are largely governed by the physical and chemical properties of the surfaces, with the bulk viscosity of the fluid having little to no effect.[34] Moreover, the coefficient of friction within boundary lubrication remains invariant over a range of fluid viscosities, articulating speeds, and opposing forces.

Between the two extrema of fluid and boundary is mixed lubrication. In mixed lubrication, surface asperities and the bulk fluid share the frictional load support. Friction coefficients show the greatest dependence on bulk fluid viscosity, opposing normal pressure, and articulating

speeds during mixed lubrication. Mixed lubrication occurs when separation distances of articulating materials are approximately equal to the mean surface roughness.

1.2.2 Cartilage lubrication. As discussed previously, the biphasic frictional behavior of articular cartilage allows it to have relatively low friction coefficients while the interstitial fluid is pressurized.[12] As the fluid dissipates, friction coefficients rise approaching equilibrium and its frictional behavior becomes more dependent on the physical and chemical properties of the surrounding synovial fluid and the ECM components at the articular surface. Uncompressed cartilage tissue typically reaches equilibrium at times on the order of tens of minutes[8] depending on the relative size, health, and loading conditions of the tissue.

Once tissue relaxation occurs and the interstitial fluid pressure dissipates, the frictional behavior of articular cartilage becomes independent of time and can be more easily studied using Stribeck analysis. The frictional properties of the relaxed cartilage tissue depend on the constituents of the surrounding synovial fluid and of the articular surface. HA is found both within cartilage tissue and in synovial fluid, and has been shown to effectively lubricate cartilage surfaces. The main viscosity determinant of synovial fluid[38], HA exhibits viscoelastic behavior where it behaves as a viscous liquid at low shear rates and an elastic solid at high shear rates. Moreover, this viscoelastic behavior is compromised in OA where the concentration and molecular weight of HA are reduced.[39] Reintroducing HA into joints increases synovial fluid viscosity[40], effectively altering lubrication mode toward mixed or fluid lubrication. However, the mode of lubrication with the highest friction coefficients and incidence of wear is boundary lubrication. This potentially explains the limited efficacy of HA viscosupplementation on treating OA progression. Furthermore, a glycoprotein protein later named lubricin was found in synovial fluid to provide boundary lubricating properties, not HA.[40,41]

1.3 Lubricin

Lubricin, a mucinous glycoprotein localized in synovial fluid and on the surface of articular cartilage[42], is an effective boundary lubricant of cartilage. Lubricin reduces the equilibrium friction coefficient in boundary lubrication by as much as 70-percent.[41] Furthermore, the addition of lubricin to injured cartilage mitigated tissue degradation, slowing cartilage damage progression by up to 83-percent in some cases.[43–49] The restoration of friction properties and amelioration of tissue damage demonstrates the molecule's significant therapeutic potential.

This potent lubricating ability arises from the structure of lubricin. (Figure 1.3) The glycoprotein has a molecular weight of 280 kDa, and is approximately 200 nm in length.[50] The central mucin domain consists of a core protein of approximately 120 kDa[50] surrounded by a dense hydrophilic oligosaccharide brush. The C-terminus of lubricin binds the protein to the cartilage surface, whereas the N-terminus controls aggregation.[51] It is believed that these structures work together providing the lubricating mechanism of lubricin.[52] The C-terminus anchors the molecule to the cartilage surface[53], while the oligosaccharides of the mucin domain attract and retain water near the molecule[54]. On a surface populated by lubricin molecules such as that of articular cartilage, a network of these glycoproteins forms that in turn promotes the formation of an aqueous film near the surface that facilitates movement and reduces friction even at instances of high opposing forces such as in boundary friction.

However, substantial barriers that hinder the widespread use of lubricin as a therapy for joint injury are the challenges in producing recombinant versions of the molecule. Bacterial and insect cell lines cannot produce lubricin due to its high degree of glycosylation, and mammalian cell lines have also failed to reliably produce full-length lubricin.[43] Production of lubricin from Chinese hamster ovary cell lines generates molecules with truncated mucin domains containing a

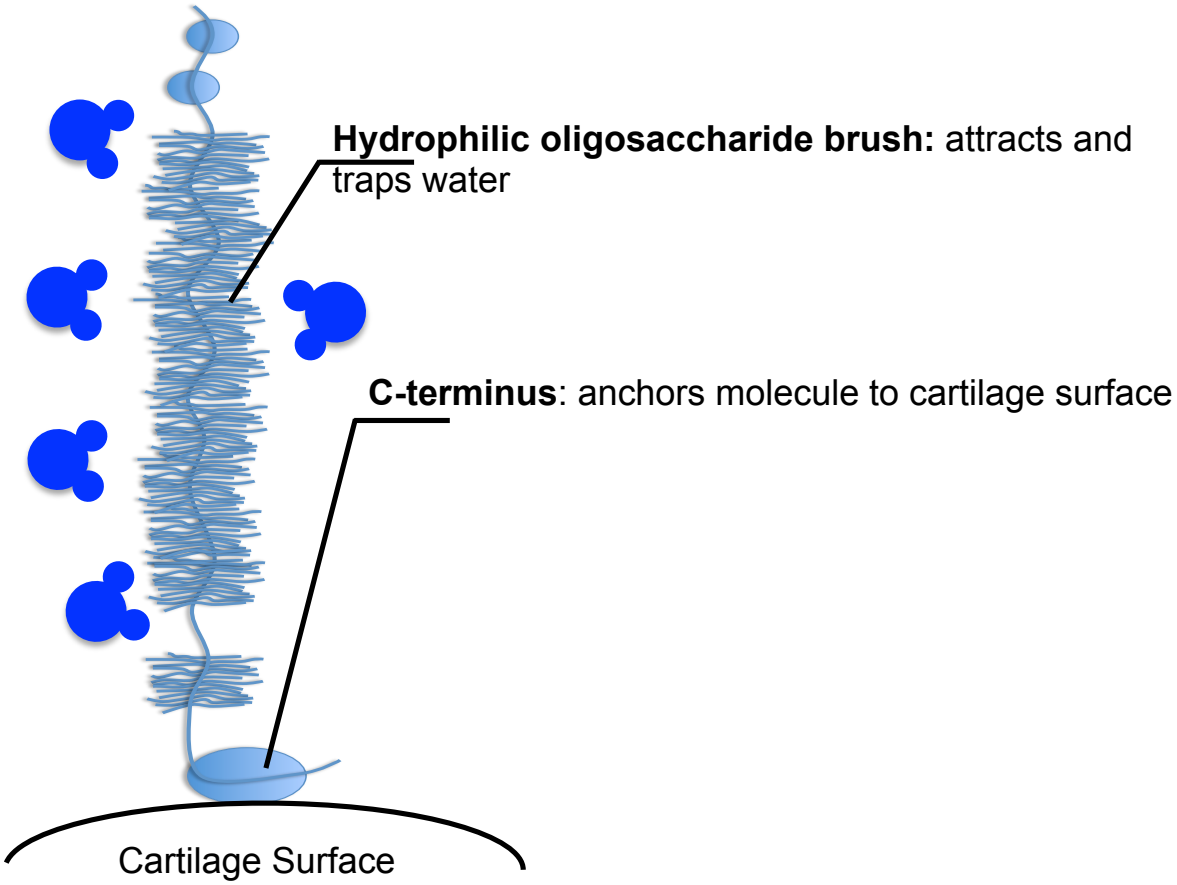

Figure 1.3. The lubricating action of lubricin stems from its lubricating mucin domain and binding C-terminus. A populace of lubricin on the articular surface promotes the formation of an aqueous film, facilitating movement and lowering friction

peptide sequence about one-third of the length of those of full-length human lubricin.[43] This new form of lubricin, LUB:1, was shown to lubricate articular cartilage in boundary lubrication, but was less effective than full-length lubricin.

Investigations into lubricin's therapeutic potential have resulted in mechanical and biological evidence of chondroprotection. Mechanically, lubricin reduces the boundary friction coefficients[41] of cartilage and prevents wear and damage progression[55]. Biologically, lubricin has demonstrated the ability to mediate cell adhesion[56] and to bind and signal through CD44 receptors on chondrocytes and synoviocytes[57]. Intra-articular injection of lubricin into injured joints has also shown to be both mechanically and biologically chondroprotective. (Table 1.1)

1.4 Synthetic lubricants

1.4.1 Synthetic boundary lubricants. Since the proposed lubricating mechanism depends solely on lubricin's structure, the glycoprotein has been used as a template to create synthetic boundary lubricants. A synthetic lubricin would have two contributing domains: a C-terminus mimic that binds the molecule to an articulating surface and a lubricating mucin-like domain that keeps the surface hydrated. Molecules made to mimic these attributes of lubricin should demonstrate similar lubricating effects.

Tunable polymer brush structures were synthesized with poly(L-lysine) (PLL) backbones grafted with either poly(ethylene glycol) (PEG)[58] or dextran[59]. Both the PLL-graft-PEG and PLL-graft-dextran structures were effective boundary lubricants of oxidized surfaces. The negatively charged PLL backbone adhered to the positively charged substrates, and the brush layer kept them hydrated forming a lubricating aqueous film. By changing the substrate material, the degree of PLL adsorption was changed.

Table 1.1. Intra-articular treatment of injured Lewis rats with lubricin

Authors	Lubricin	Injury	Chondroprotective evidence
Elsaid+[49]	Purified Human Synoviocyte Lubricin (HSL)	Anterior Cruciate Ligament Transection (ACLT)	• Lower OARSI scores • Lower uCTXII levels • Higher lubricin expression
Vugmeyster+[48]	LUB:1	Meniscal Tear (MT)	• Localization on damaged sites
Jay+[46]	HSL	ACLT	• Lower uCTXII levels • Better gait symmetry
Teeple+[44]	HSL	ACLT	• Lower OARSI scores • Higher levels of lubricin in synovial fluid lavages
Jay+[45]	HSL; recombinant lubricin	ACLT	• Lower OARSI scores • Lower uCTXII levels
Flannery+[43]	LUB:1	MT	• Lower friction coefficients • Smaller lesion size • Reduced cell adhesion • Lower histology grades

With half of the relative polymer adsorbed, friction coefficients were approximately doubled. Binding of the lubricants to an articulating surface is essential for the boundary lubricants to effectively lubricate. By manipulating the size of the PEG brushes, the hydrophilicity of the lubricants and thickness of the lubricating film could be modulated. Larger PEG chains resulted in lower friction coefficients. Interestingly, the PLL-graft-PEG was also a significantly better lubricant than PLL-graft-dextran, despite dextran being a hydrophilic polysaccharide that more closely resembling the oligosaccharides of lubricn.

Other synthetic boundary lubricants have used other binding conformations to achieve lubrication. Most notably, alkanethiols were self-assembled onto gold-coated substrates.[60] These thiols were designed to exhibit different packing densities and showed that the frictional properties of the modified surface depended on the packing of the polymer network. Doubling the packing density resulted in increased hydrophilicity and a decrease of friction coefficients by approximately 70 percent.

In summary, the efficacy of the boundary lubricants depended on (1) their ability to securely bind to the surface, (2) the hydrophilicity and lubricating film thickness, and (3) the packing density of the molecules on an articulating surface.

1.4.2 Synthetic cartilage lubricants. There have also been efforts to synthetically lubricate cartilage. One such group created a large molecular weight anion that is able to reduce friction by increasing fluid viscosity[61], moving the system more towards mixed and fluid lubrication and essentially acting as a synthetic HA and likely would see the same limitations as a viscosupplement for treating OA.

In an attempt to lubricate cartilage within boundary lubrication, PEG chains were used to link collagen and HA binding peptides, which allowed for the tethering of HA to the collagen fibers

on the cartilage surface.[62] While this development is promising, the boundary lubricating effects of this methodology remains to be seen as the friction setup saw similar decreases in friction as with unbound HA in a similar system under similar conditions.[63]

1.5 Research Objectives

In summary, OA is a painful and debilitating disease that strips articular cartilage of its role as a low friction surface that prevents joint damage. Current treatments of OA have thus far proved to be ineffective. The glycoprotein lubricin, however, has exhibited the ability to restore the lubricating properties of articular cartilage and protect it from damage. Lubricin's boundary lubricating and chondroprotective abilities demonstrate its therapeutic potential for treating joint injury and cartilage diseases such as OA. Unfortunately, lubricin is difficult to produce and obtain. The lubricating mechanism of lubricin is solely dependent on its structure, and many synthetic lubricants have been modeled after the glycoprotein. None of these lubricants have demonstrated either the ability to lubricate cartilage in boundary lubrication or to prevent the progression of cartilage damage. Thus, the central goal of this work is to develop and characterize a library of synthetic lubricin-mimetics that effectively bind to, lubricate, and protect cartilage.

The research accomplished in this dissertation was done in collaboration with Mingchee Tan of the Putnam Laboratory at Cornell University. Tan was able to mimic the molecular composition and function of native lubricin, designing and synthesizing brush-like copolymers to impart both cartilage binding and hydrogen bonding domains. Specifically, PEG chains were grafted to a poly(acrylic acid) (pAA) core to mimic the central mucin domain of lubricin. A thiol terminus permitted binding of the lubricants to articulating substrates. These brush copolymers

were modular in design, where the configurations and potentially their lubricating ability could be controlled by changing the pAA core size, PEG chain size, or the PEG chain density.

1.5.1 Specific Aim 1 (Chapter 2): To test the hypothesis that synthetic copolymer brushes with tunable lubricating and binding domains analogous to the structures of lubricin effectively and predictably reduce boundary friction coefficients of cartilage.

A family of biomimetic boundary lubricants was synthesized mimicking the brush-like structure of the natural glycoprotein lubricin. These polymers were engineered with tunable lubricating domains, and different polymer configurations were synthesized using different backbone and hydrophilic brush sizes. Hydrodynamic size of the brush-like copolymers increased with backbone length and brush length. The lubricin-mimetics had a thiol terminus that was used to bind to gold coated substrates, on which characteristics of each polymer network were found. Once bound, the lubricin-mimetics demonstrated significant lubricating ability when tested against articular cartilage. Furthermore, correlations were observed between hydrodynamic size, globule size, mean surface roughness, and lubrication, all suggesting that larger boundary lubricants lubricate better. While the lubricin-mimetics in the polymer library did not achieve the same level lubrication as lubricin, boundary lubricants of similar hydrodynamic size to lubricin would potentially approach its lubricating efficacy.

1.5.2 Specific Aim 2 (Chapter 3): To test the hypothesis that biomimetic polymers with structures analogous to both the binding and lubricating domains of lubricin will be effectively bind to and lubricate articular cartilage.

A family of biomimetic boundary lubricants was synthesized mimicking the brush-like structure of the natural glycoprotein lubricin and its ability to bind to and lubricate cartilage surfaces. With a thiol-terminated core, these lubricin-mimetics were able to adhere to the

articular surface of cartilage, and because of this attachment they effectively lubricated the cartilage surfaces. The lubricin-mimetics differed in backbone size, brush size, and brush density. Increases in any of these three structural variables directly led to molecules with larger hydrodynamic size and longer binding time constants. All binding time constants were below 40 min, well below the clearance times of synovial fluid. This suggests, if introduced in vivo, the lubricin-mimetics will bind to the cartilage before being expelled from the joint. The different polymer configurations provided different boundary friction coefficients, but no inference was able to be made linking polymer configuration and lubricating ability. While no polymer lubricated as effectively as lubricin, six of the eight lubricants effectively lubricated cartilage. Two of which did so more effectively than LUB:1, a lubricin mutant that has previously demonstrated chondroprotective ability. With their significant lubricating ability, the lubricin-mutants show potential to preserve the lubricating properties of cartilage and prevent the progression of damage in joints.

1.5.3 Specific Aim 3 (Chapter 4): To test the hypothesis that a synthetic brush copolymer with analogous structures to lubricin that effectively binds to and lubricates cartilage can prevent cartilage damage in vivo.

The lubricin-mimetic that demonstrated the greatest lubricating capacity also preserved the frictional properties and surface morphology of cartilage while preventing the progression of joint damage in a rat knee model of OA. The lubricin-mimetic displayed significant chondroprotective ability, lowering OARSI scores by approximately the same decrement as lubricin in a similar OA injury model. Joints treated with the lubricant were smoother and had lower friction coefficients than those left untreated. This study presented qualitative, quantitative, and functional evidence of a lubricin-mimetic exhibiting significant chondroprotective ability.

The data strongly encourages the further development of this biomimetic copolymer as a potential therapy for cartilage injury or disease.

1.5.4 Specific Aim 4 (Chapter 5): To test the hypothesis that the lubricating capacity of biomimetic polymers with structures analogous to lubricin tested against cartilage in an in vitro system will be a good indicator of the lubricant's chondroprotective ability in vivo.

Lubricin-mimetic synthetic lubricants displayed the ability to lubricate and protect cartilage to varying degrees, and demonstrated chondroprotective ability can be predicted by using an in vitro tribometric system. Better lubricants displayed better chondroprotective ability, providing a method for screening potential OA treatments for future animal trials. This study develops the basis for a screening process for cartilage boundary lubricants as potential injury therapeutics. The chondroprotective ability of a boundary lubricant can be predicted by its boundary lubricating capacity. This further elucidates the mechanisms behind chondropotection of cartilage, but could also save considerable expense and labor in preventing additional animal trials for lubricants that were not.

2.0 Tunable lubricin-mimetics for boundary lubrication of cartilage.

2.1 Abstract

The glycoprotein lubricin is the primary boundary lubricant of articular cartilage. Its boundary lubricating abilities arise from two key structural features: i) a dense mucin-like domain consisting of hydrophilic oligosaccharides and ii) an end terminus that anchors the molecule to articulating surfaces. When bound, lubricin molecules attract and trap water near a surface, reducing friction and facilitating glide. In this study, synthetic analogues were created to mimic lubricin using thiol-terminated polyacrylic acid-*graft*-polyethylene glycol (pAA-*g*-PEG) brush copolymers. The PEG moiety was designed to mimic the mucin-like domain of lubricin and the thiol terminus was designed to anchor the molecules to gold-coated surfaces, mimicking the binding domain. A library of nine copolymer brushes was synthesized using different sizes of pAA and PEG. Larger molecular weight polymers created smoother, more densely covered surfaces ($p<0.05$). Additionally, the hydrodynamic sizes of the polymers in solution were correlated with their lubricating abilities ($p<0.05$). Friction coefficients of cartilage against polymer-treated gold surfaces were lower than cartilage against untreated surfaces ($\Delta\mu_{eq}$= -0.065±0.050 to -0.093±0.045, $p<0.05$). In summary, pAA-*g*-PEG copolymers efficiently replicated the lubricating properties of lubricin demonstrating their potential use for future treatment of joint diseases such as osteoarthritis.

2.2 Introduction

One of the primary functions of articular cartilage is to provide a low friction surface for diarthrodial joints. Lubrication of these joints depends on a variety of factors, most notably on synovial fluid and its constituents.[63] Lubricin, a mucinous glycoprotein found in synovial fluid and on the surface of articular cartilage[64], is an effective boundary lubricant. Lubricin reduces the boundary mode friction coefficient by as much as 70%.[41] Furthermore, the addition of lubricin to injured cartilage mitigates tissue degradation, slowing cartilage damage progression by up to 83% in some cases.[43] The restoration of friction properties and amelioration of tissue damage demonstrates lubricin's significant therapeutic potential.

This potent lubricating ability arises from the structure of lubricin. The glycoprotein has a molecular weight of 280 kDa, and is approximately 200 nm in length.[42] The central mucin domain consists of a core protein surrounded by a dense hydrophilic oligosaccharide brush.[50] The C-terminus of lubricin binds the protein to the cartilage surface, whereas the N-terminus controls aggregation.[56] It is believed that these structures work together to provide the lubricating mechanism of lubricin.[52] The C-terminus anchors and orients the protein at the cartilage surface, while the oligosaccharides of the mucin domain attract and retain water near the molecule. Collectively, these characteristics promote the formation of an aqueous film proximal to the cartilage surface, facilitating glide and reducing friction even under high normal loads or low velocities such as in boundary friction.

However, lubricin is highly glycosylated with tandem repeating units, which makes its recombinant synthesis challenging and limits its widespread use as a therapy for joint injury. Previous work shows that mammalian cell lines frequently produce truncated forms of lubricin.[56] More specifically, the expression of lubricin from Chinese hamster ovary cell lines generates

molecules with truncated mucin domains containing a peptide sequence about one-third of the length of those of full-length human lubricin.[43] This new form of lubricin, LUB:1, lubricates articular cartilage in boundary lubrication, but to a lesser degree than full-length lubricin.

Because the proposed lubricating mechanism of lubricin depends solely on its structure, synthetic molecules made to mimic these attributes of lubricin demonstrate similar lubricating effects. Mucin-inspired co-polymer brushes act as aqueous boundary lubricants in non-biological systems.[58,65–67] Similarly to lubricin, synthetic mucins have two contributing features: a binding terminus for attachment to an articulating surface and a hydrophilic lubricating domain to maintain surface hydration.

To address the hypothesis that synthetic polymer brushes can mimic the function of lubricin, a series of such materials, specifically polyacrylic acid-*graft*-polyethylene glycol (pAA-*g*-PEG), was synthesized (Figure 1). The pAA backbone length and PEG molecular weight were altered to determine how these parameters correlated to lubrication. The pAA was terminated with a free thiol group to allow facile attachment to gold surfaces.[60]

The goal of this study was to gain a greater understanding of how the molecular architecture of lubricin-mimetics correlate to lubrication under boundary conditions. The specific objectives were to (1) describe and synthesize a series of synthetic lubricants that mimic the structure of lubricin; (2) examine the physical characteristics of these lubricants in solution and on idealized surfaces; and (3) determine the ability of these polymers to lubricate cartilage.

2.3 Materials and methods

2.3.1 Synthesis of lubricin-mimetics: According to the proposed lubrication mechanism, the moieties of lubricin most responsible for boundary lubrication are its C-terminus, which controls

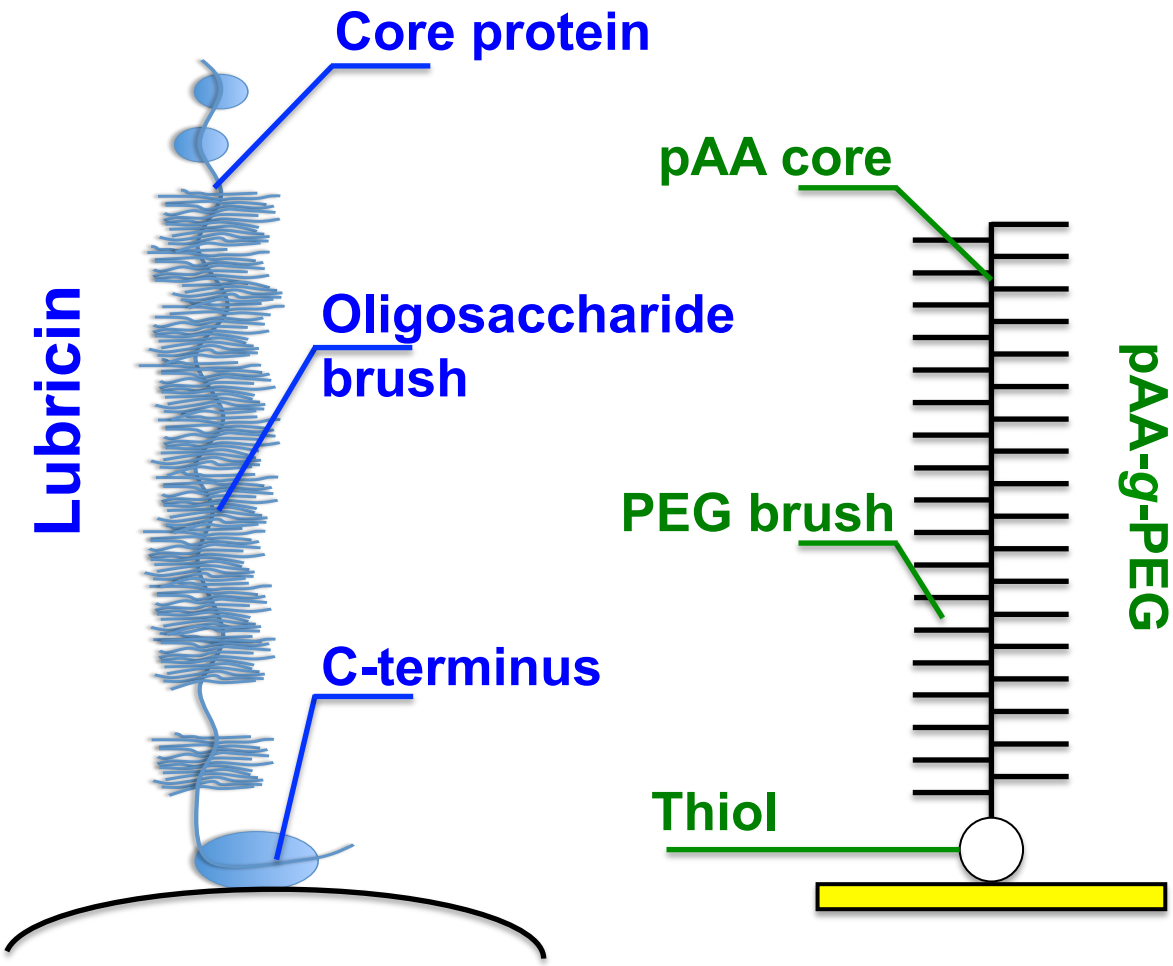

Figure 2.1. Schematics of lubricin (left) and the pAA-*g*-PEG mimetic (right) are shown. Both configurations have a hydrophilic brush and an end terminus that anchors the molecules to surfaces

binding to surfaces, and its hydrophilic mucin domain, which attracts water. To mimic the brush-like mucin domain, hydrophilic polyethylene glycol (PEG) brushes were grafted to a polyacrylic acid (pAA) core. The pAA was synthesized via reversible addition−fragmentation chain-transfer (RAFT) polymerization using acrylic acid (AA), 4,4′-azobis 4-cyanopentanoic acid (A-CPA) and 4-cyanopentanoic acid dithiobenzoate (CPA-DB) under anhydrous, airtight and dark conditions.[70] The AA concentration was maintained at 3 mM while varying the concentrations of A-CPA and CPA-DB. A typical reaction scheme is as follows: AA (950 µl) was added to a flame dried 5 ml brown ampule with magnetic stirrer. Then CPA-DB (5.3 mg) was dissolved in nitrogen-purged methanol (2.9 ml) and added into the ampule containing AA. A-CPA (1.3 mg) was dissolved in 0.7 ml of nitrogen-purged methanol and added into the reaction ampule. Nitrogen gas was bubbled through the reaction mixture during and after the addition of each reagent for several minutes to prevent oxygen gas diffusion. Following the final nitrogen purge, the ampule was flame-sealed and placed in a 60°C oil bath to initiate polymerization. After 48 hours, the ampule neck was broken, and the reaction was exposed to air and cooled on ice to stop further reaction. The solution was then diluted and dialyzed against deionized water for 3 days and lyophilized to obtain a white, waxy powder.

The pAA-*graft*-PEG copolymer was synthesized via conjugation chemistry using 4-(4,6-dimethoxy-1,3,5-triazin-2-yl)-4-methyl morpholinium chloride (DMTMM) as the coupling agent based on a procedure developed previously.[71] An example reaction is as follows: pAA (10 mg, M_W 107,600) and PEG-amine (0.151 g, M_W 2,000) were dissolved and mixed together in 2.4 ml of 0.1 M borate buffer (pH 8.5) in a 10 ml flask with stir bar. DMTMM (19.2 mg) dissolved in 0.6 ml of 0.1 M borate buffer was then added drop-wise to the mixture and pH was adjusted to 6-

7 using 1 N HCl. The reaction was allowed to progress for 24 hours and then dialyzed against deionized water for 3 days, before being lyophilized to recover a white powder.

2.3.2 Characterization and attachment of lubricin-mimetics: A series of copolymers with varied core and brush lengths was created to characterize their behavior both in solution and on surfaces. To characterize the behavior of the mimetics in solution, the hydrodynamic size each polymer was measured via dynamic light scattering. pAA-*graft*-PEG copolymers were dissolved in filtered 1 M PBS at a concentration of 3 mg/ml, and hydrodynamic diameters were measured using a Malvern Zetasizer Nano ZS at 20°C and a detector angle of 173°C.

Next, the lubricating efficacy of the mimetics were assessed by anchoring them to gold substrates. Several studies have examined the formation of self assembled monolayers through the use of thiol-gold interactions.[60,72,73] The thiol terminus of the lubricin-mimetics bound to gold-coated glass slides, facilitating friction evaluation. Using a Varian Bell Jar Thermal Evaporator under a vacuum of approximately 10^{-7} Torr, a 10 nm-thick chromium layer and a subsequent 20 nm-thick layer of gold were deposited on polished glass slides. Each polymer was dissolved in deionized water (3 mg/ml) and incubated on the gold surfaces for at least 24 hours. The surfaces were then rinsed with deionized water to remove any unbound polymers.

Four polymer architectures (pAA sizes of 60 and 105 kDa, PEG sizes of 2 and 10 kDa) were used to characterize the extent of surface modification by the lubricin-mimetics. These four mimetics were chosen for their distinct differences in brush characteristics to better elucidate distinct structure-function relationships. The gold-treated glass substrates were imaged while hydrated on an Agilent PicoPlus atomic force microscope (AFM) using silicon oxide tips mounted on 0.3 N/m cantilevers (Bruker), and subsequently analyzed with Gwyddion software.

2.3.3 Cartilage lubrication: Full thickness patellofemoral groove cartilage was removed from one to three day old bovine calves with a scalpel, and subsequently frozen and stored at -20°C.[41] At the time of testing, the tissue was thawed in a water bath at 37°C. A biopsy punch and a scalpel were used to create 6 mm diameter by 2 mm thick discs maintaining the articular surface. The discs were immersed in a 1.5 M NaCl solution for 30 minutes to remove native lubricin from the surface without affecting the collagen or proteoglycan structure.[56,74] Cartilage samples were then immersed in PBS for 60 min to restore osmotic equilibrium.

Cartilage discs and glass slides were loaded into a custom cartilage-on-glass tribometer described previously.[56] For these experiments, the cartilage was tested against gold-coated glass slides loaded into the tribometer. An initial compressive normal strain of 40% was induced onto each cartilage disc; one hour was given to allow the cartilage to reach mechanical equilibrium under this compressive strain. The tribometer was then used to linearly oscillate the cartilage discs against the slide surfaces at an entraining speed of 0.3 mm/s, conditions known to be well within boundary lubrication for this system.[41] The time-dependent normal and shear loads were measured, and the friction coefficient of each sample was calculated from the ratio of the shear to the normal loads, $\mu_{eq} = F_{shear}/F_{normal}$. The change in friction coefficients compared to unlubricated controls, $\Delta\mu_{eq}$, was used to assess lubricant lubricity. The temporal patterns observed were similar to those seen previously for boundary lubrication of cartilage on glass.[41,75]

Five slides of each polymer were prepared. Five control slides were also prepared with a gold film deposition, but without any polymer treatment. Each slide was only used for one friction test. A different cartilage disc was tested against each prepared slide.

2.3.4 Statistics. A two-way ANOVA was used to compare the effects of pAA size and PEG size on surface characteristics. Linear regressions were used to analyze relationships between the

means of the hydrodynamic sizes, surface characteristics, and the lubricating abilities of the polymers.

2.4 Results

2.4.1 Synthesis. A library of lubricin-mimetics was created with a range of backbone sizes and brush sizes (Table 1). Sizes of the pAA backbones ranged from M_W 60 to 145 kDa, while sizes of the PEG side chain ranged from M_W 2 to 10 kDa. Varying both backbone and brush length provided a library of nine biomimetic lubricants.

By changing these two parameters, the contour length, diameter, and hydrodynamic size of the lubricants were controlled. Hydrodynamic sizes of the polymers increased with pAA and PEG length and ranged from 47 to 111 nm, compared to 173 nm for lubricin[64], and 62 nm for LUB:1[43,64].

2.4.2 Surface coverage. To evaluate the effect of each of the structural parameters varied in this study (M_W of pAA and PEG), four lubricin-mimetics were used. The mimetics varied in pAA size (105 kDa and 60 kDa) and PEG size (10 kDa and 2 kDa). Gold-coated slides treated with the four different mimetics were imaged via AFM. Polymers of different molecular architectures and sizes had unique surface coverage patterns. Quantification and characterization of the AFM images of the gold-coated surfaces was conducted by determining the average surface roughness (R_a), the mean globule sizes, the fraction of area covered by polymer globules, and the peak-to-peak distances between the globules (Figure 2). Larger polymers resulted in greater and more complete surface coverage. The mean globule size and mean coverage area increased with pAA backbone size ($p<0.05$). The effect of PEG size was less pronounced ($p=0.16$). Mean globule sizes for the mimetic-treated slides ranged from 31.5 to 62.6 nm, and the mean coverage area of

Table 2.1. Polymer Configuration and Size

pAA Size (kDa)	PEG Size (kDa)	Hydrodynamic Size (nm)
60	2	47
60	5	67
60	10	91
105	2	81
105	5	103
105	10	105
145	2	84
145	5	89
145	10	111

Lubricin Core (kDa)	Brush Size (kDa)	Hydrodynamic Size (nm)
120[14]	0.4-2.3[6,15]	173[2]

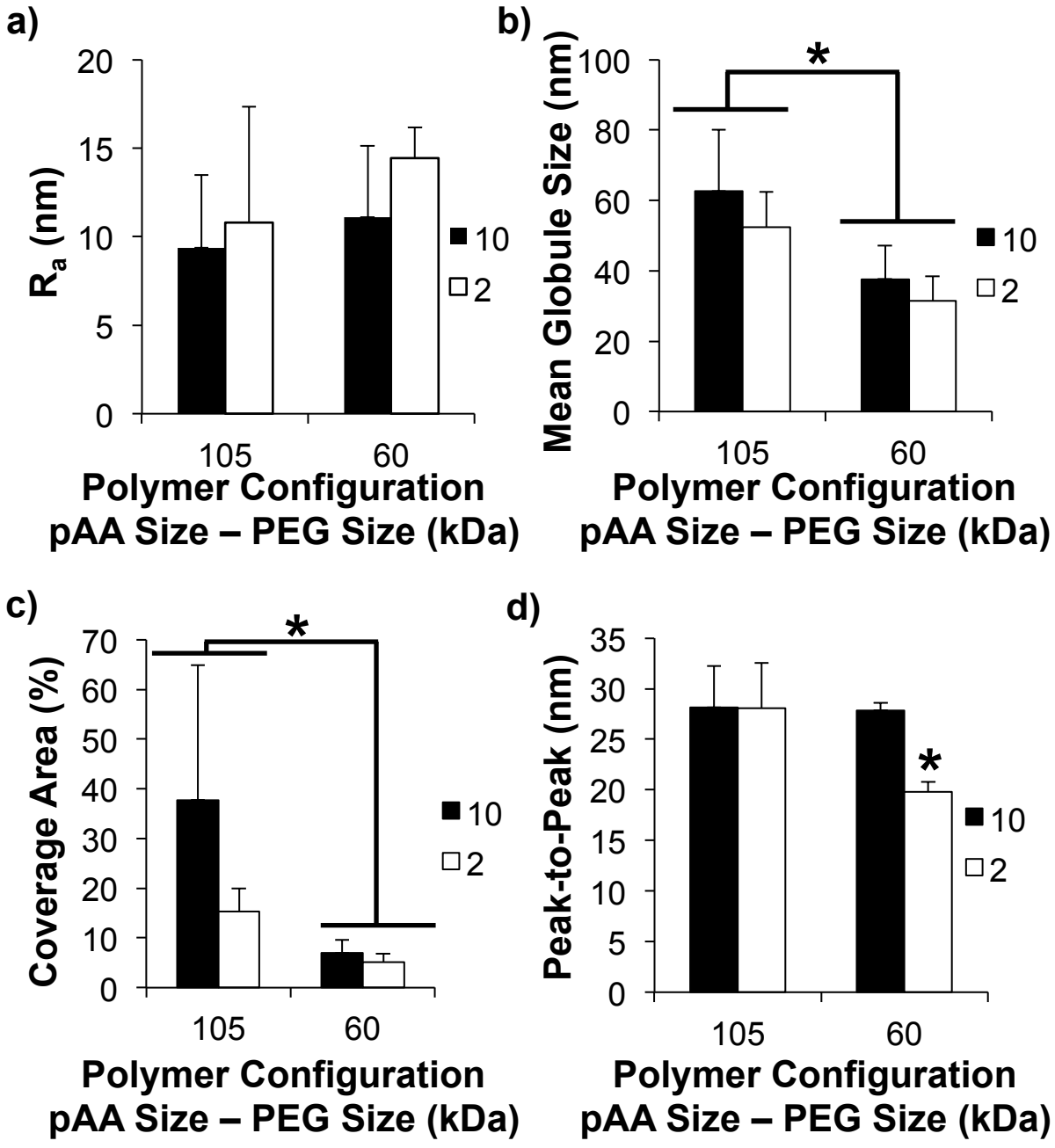

Figure 2.2. The depositions of the polymers on gold surfaces are characterized by **a)** surface roughness, **b)** mean globule size, **c)** coverage area, and **d)** peak-to-peak distances. No difference was seen in the surface roughness characteristics, whereas polymers with larger pAA size formed films with larger globules and more coverage ($p<0.05$). Interestingly, the smallest polymer covered the least area but still had the highest packing density (lowest peak-to-peak distances, $p<0.05$).

the polymers on the gold surfaces ranged from 5.2 to 37.8%. The peak-to-peak distance metric is a measure of the number density of the polymers or globules formed on a surface. The peak-to-peak distances between globules for the surface layers formed by the three larger polymers varied minimally, whereas the mean peak-to-peak distance for pAA(60)-*g*-PEG(2) was significantly lower ($p<0.05$).

The hydrodynamic size of the different lubricin-mimetics is a metric of how the molecules behave in solution. To better understand the relationships between the behaviors of the mimetics in solution and at surfaces, their surface characteristics were compared to their hydrodynamic sizes (Figure 3). Polymers of larger hydrodynamic size had larger globule sizes that covered more area, providing lower surface roughness ($p<0.05$) despite having lower packing densities ($p<0.05$). Polymers with larger hydrodynamic sizes formed thicker and more complete networks on surfaces, characteristics previously shown to provide better boundary lubrication.

2.4.3 Lubrication. To better understand how the lubricating functionality of the polymers on surfaces relates to their behavior in solution, the experimental library was expanded to nine mimetics. Each of the nine lubricin-mimetics effectively lubricated articular cartilage. Equilibrium coefficients of friction of the cartilage plugs were significantly lower ($p<0.05$) in the presence of biomimetic polymers compared to controls lubricated by PBS alone, with the change, $\Delta\mu_{eq}$, ranging from -0.065±0.050 to -0.093±0.045. Although no statistical relationship was found between the measured surface characteristics and the lubricating abilities of the mimetic-modified slides ($p=0.21$-0.43), the lubricating ability correlated well with the mimetics' hydrodynamic size ($p<0.01$), with larger polymers lubricating more effectively (Figure 4). This further suggests that the lubricin-mimetics with larger hydrodynamic sizes promoted the formation of thicker lubricating aqueous films.

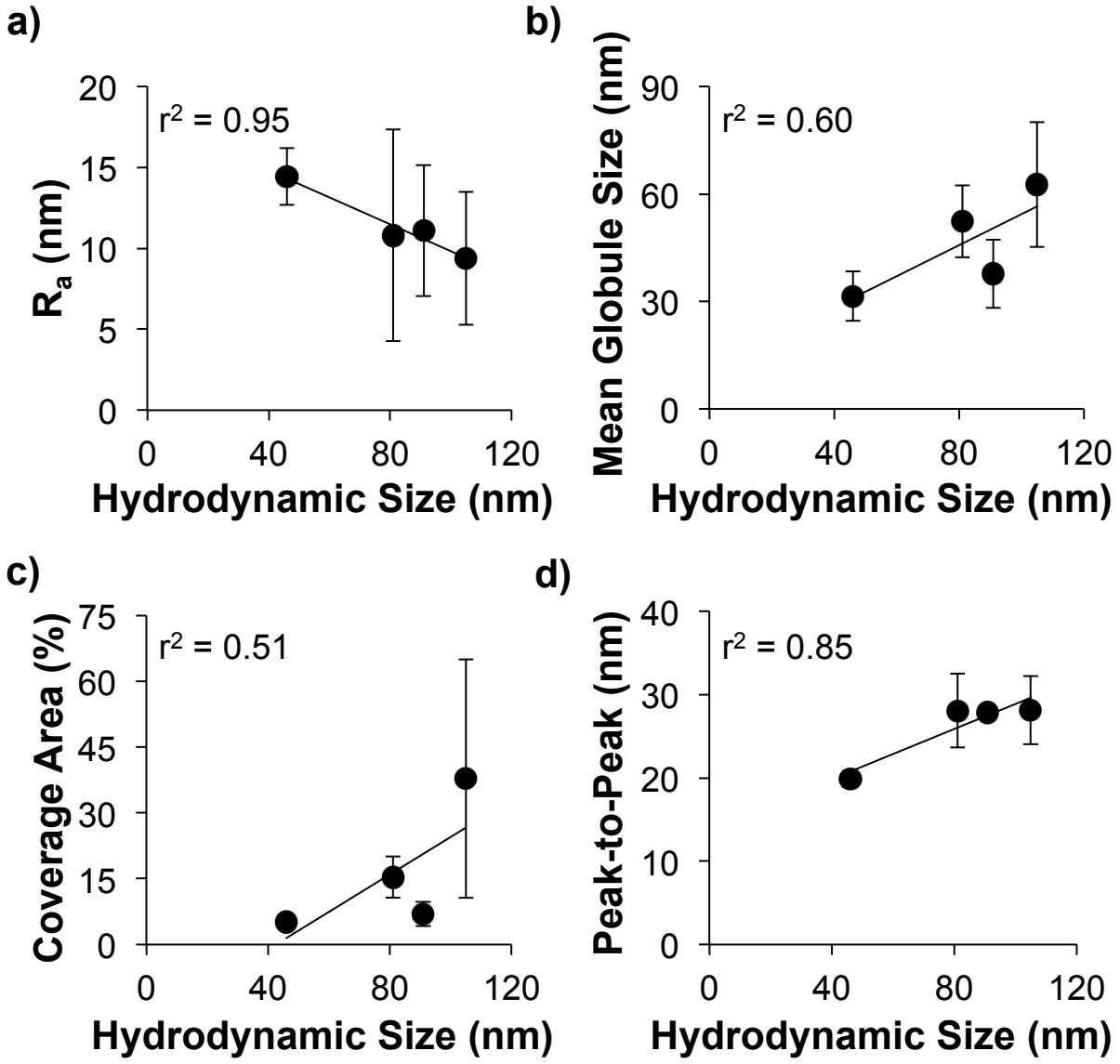

Figure 2.3. The surface characteristics **a)** surface roughness, **b)** mean globule size, **c)** coverage area, and **d)** peak-to-peak distances are compared to the larger hydrodynamic sizes of the molecules. Polymer configurations of larger hydrodynamic size tended to form surfaces of lower surface roughness despite having lower packing densities.

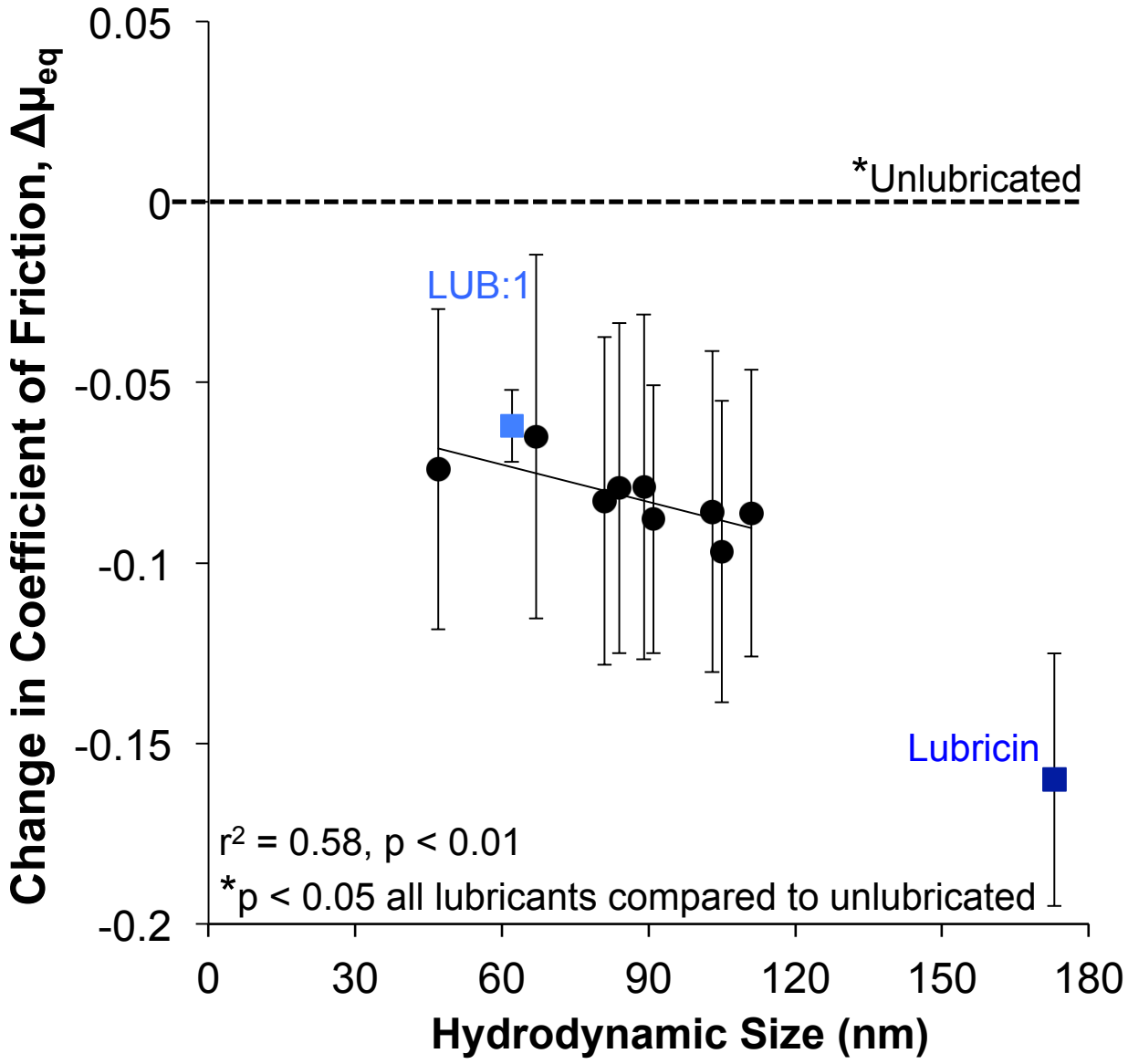

Figure 2.4. The lubricin-mimetics effectively lubricated cartilage; the coefficients of all four polymers were significantly lower than that of the unlubricated case. Although none of the polymers approached the lubricating ability of lubricin[2,3], they were comparable to that of LUB:1[2,4]. An observed trend indicates that a polymer's lubricating ability increases with hydrodynamic size. Values obtained from the literature for lubricin and LUB:1 are consistent with this trend. Additionally, pAA-*g*-PEG brush polymers of similar hydrodynamic size to that of lubricin could potentially lubricate as effectively.

While the lubricin-mimetics significantly lowered friction coefficients, the previously measured[41] $\Delta\mu_{eq}$ of cartilage in the presence of native lubricin, -0.16±0.035, was still lower than that of any of the biomimetic lubricants. The polymers also did not achieve the hydrodynamic size of lubricin (173 nm), with the largest being 111 nm. Additionally, the $\Delta\mu_{eq}$ of LUB:1[43], -0.060±0.010, was comparable to that of lubricin-mimetics of similar hydrodynamic size. Larger polymers also lubricated more effectively than LUB:1, which has been shown to prevent the progression of cartilage damage. Looking to future work, the lubricin-mimetics with larger hydrodynamic sizes lubricated more effectively; therefore an increase in hydrodynamic size through a combination of an increase in pAA and/or PEG may lead to lubricin-mimetics with comparable hydrodynamic sizes and lubricating ability of lubricin.

2.5 Discussion

In this study, a family of biomimetic boundary lubricants was synthesized to mimic the brush-like structure of the natural glycoprotein lubricin. The behavior of these molecules in solution was characterized via dynamic light scattering. The hydrodynamic sizes of the brush-like pAA-*g*-PEG copolymers increased with pAA backbone length and PEG brush length. These lubricin-mimetics demonstrated significant lubricating ability when tested against articular cartilage. The equilibrium coefficient of friction, μ_{eq}, was significantly lower in the presence of biomimetic polymers compared to unlubricated controls; $\Delta\mu_{eq}$ was as low as -0.093±0.045 ($p<0.01$), lower than that for LUB:1 ($\Delta\mu_{eq}$=-0.060±0.010). Using lubricin as a template, boundary lubricants that effectively lubricated articular cartilage were created.

The lubricin-mimetics were designed to modify the gold surfaces by creating a lubricating film, and the different mimetics resulted in surfaces with different characteristics. Polymers with

larger pAA backbone sizes resulted in the formation of larger globules and denser coverage area. Larger polymers formed surfaces with more lubricant coverage to better promote the formation of lubricating films, facilitating movement, and lowering friction.

Additionally, clear correlations between the behavior of he mimetics in solution and on surfaces were observed. Polymers with larger hydrodynamic sizes formed smoother surfaces. This reinforces the idea that polymers that are larger in solution form smoother and more complete lubricating films on surfaces, and in turn enhance lubrication. Moreover, larger hydrodynamic sizes also suggest that the resultant film created on a surface would be thicker allowing for greater separation of articular surfaces, which also promotes the reduction of friction. Interestingly, the smallest polymers had better number packing density but the lowest coverage area fractions. While these smaller lubricants pack more densely, they would form a thinner lubricating film and possibly a less complete network of lubricating brushes than their larger counterparts due to the discontinuity in total area covered.

A correlation was observed where $\Delta\mu_{eq}$ decreased as the hydrodynamic size of the lubricant increased. While the $\Delta\mu_{eq}$=-0.16±0.035 for lubricin was lower than any of the synthetic lubricants tested, the hydrodynamic size of lubricin was also larger than any of the mimetic polymers synthesized. The observed trend suggests that biomimetic lubricants with large enough hydrodynamic sizes may lubricate as effectively as lubricin. Additionally, the larger polymers created smoother films allowing for better lubrication. This also reinforces the idea that larger lubricant hydrodynamic sizes correlate with thicker resultant lubricating films, and that thicker films have higher lubricity. This is consistent with other tribological studies examining boundary lubrication, including those investigating the use of PEGs to reduce friction coefficients on metal oxide and silicon oxide surfaces.[58,66,67] In these studies, poly(L-lysine)-*g*-PEG copolymers were

used to create a boundary lubricating film. Increases in PEG length increased the fluid film thickness and lubricity. By modulating the structural parameters we were able to mimic the behavior of lubricin, providing tunable, self-assembled aqueous lubrication to cartilage.

Furthermore, these results provide greater insight into how the mechanism by which lubricin functions, confirming a connection between its structure and lubrication and supporting the proposed lubrication mechanism previously described[52]. The structure of the mucin domain is largely responsible for providing lubricin with its lubricating abilities. LUB:1 was previously shown to effectively lubricate cartilage despite having a mucin domain of approximately one-third the length of lubricin. The relative size and lubricating ability of LUB:1 was comparable to the lubricin-mimetics shown, emphasizing the dependence of lubricating ability on the structure of the lubricants. This lubricating ability is largely dependent on the hydrophilicity of the brush. The polymers with larger PEG side chains had larger hydrodynamic sizes, suggesting that more PEG will lead to enhanced lubrication. Lubricin exhibits similar behavior as its hydrophilic oligosaccharides are primarily responsible for its lubricating ability. Importantly, if the sugars are removed from the core protein, lubricin's lubricating efficacy drops by as much as 77%.[50]

By mimicking the hydrophilic, brush-like structure of lubricin, pAA-*g*-PEG copolymers were effective boundary lubricants of articular cartilage. Using different pAA backbone sizes and PEG side chain sizes, the lubricin-mimetics were tuned to create surfaces of different characteristics and different lubricating abilities. In this system, pAA-*g*-PEG polymers were bound to gold surfaces by self-assembly via a terminal thiol. Applications to direct lubrication of cartilage will require interaction between the polymers and the tissue. Creation of a polymer library thus enables independent tuning of the binding and lubrication function of these materials, with the ultimate goal of developing cartilage boundary lubricant therapies.

3.0 Characterization of Binding and Lubricating Properties of Biomimetic Boundary Lubricants for Articular Cartilage

3.1 Abstract

The glycoprotein lubricin is the primary boundary lubricant of articular cartilage. In this study, a library of eight bottle-brush copolymers were synthesized that mimicked the structure and function of lubricin. PEG grafted onto a pAA core mimicked the hydrophilic mucin-like domain of lubricin, and a thiol terminus anchored the polymers to cartilage surfaces much like lubricin's C-terminus. These pAA-*g*-PEG copolymers rapidly bound to cartilage surfaces with binding time constants ranging from 20 to 39 min, and effectively lubricated them with coefficients of friction from 0.140±0.024 to 0.248±0.030. Binding and lubrication were highly correlated (r^2=0.89-0.99), showing that boundary lubrication in this case strongly depends on the binding of the lubricant to the surface. Along with time-dependent and dose-dependent behavior, lubrication and binding of the lubricin-mimetics also depended on the structural parameters pAA backbone size, PEG side chain size, and PEG:AA brush density. Polymers with larger backbone sizes, brush sizes, or brush densities took longer to bind ($p<0.05$). Six of the eight polymers reduced friction ($p<0.05$), demonstrating the potential of the lubricin-mimetics to lubricate and protect cartilage in vivo. In polymers with shorter backbones, increasing hydrodynamic size inhibited lubrication ($p<0.08$), while the opposite was observed in polymers with longer backbones ($p<0.05$).

3.2 Introduction

Osteoarthritis (OA) affects tens of millions of people in the US[19] and is characterized by the degradation of cartilage and joint tissue. Many of the current treatments for OA have shown little to no ability to curb the disease progression.[40] Recent research has been aimed at understanding the role of the glycoprotein lubricin, which shows potential as a possible therapy for treating OA and preventing the progression of cartilage damage.[43–49]

Lubricin is a glycoprotein found in synovial fluid and on the surface of articular cartilage in joints.[42] It has also been shown to be the primary boundary lubricant of cartilage[40]. Lubricin reduces friction of cartilage surfaces by as much as 70 percent.[41] In diseased or injured joints, lubricin levels are reduced[76] and friction is higher[41]. The reintroduction of lubricin into damaged joints has demonstrated chondroprotective ability, reducing the progression of cartilage damage by as much as 83 percent.[43–49]

The restoration of cartilage's lubricating properties and the ability to prevent damage progression demonstrates the potent therapeutic potential of lubricin. However, difficulty in producing recombinant versions of the protein stands as a significant barrier preventing the use of lubricin as a treatment for OA and similar diseases or injuries.[43]

The potent lubricating ability of lubricin arises from two key structures: a mucin-like lubricating domain and a binding terminus. The central mucin domain of lubricin consists of a core protein of about 200 nm long surrounded by a dense hydrophilic oligosaccharide brush with sugars ranging from 0.4 to 2.3 kDa in size.[50] The C-terminus of lubricin is a 120 peptide long sequence[51] that is responsible for binding the molecule to fibronectin and collagen at the cartilage surface[77]. The lubricating mechanism of lubricin is believed to arise from these two structural components working together [52]. The C-terminus anchors the molecule to the cartilage

surface [53], while the hydrophilic oligosaccharides attract and retain water near the articular surface [54]. A population of lubricin molecules then form a network of hydrophilic mucins anchored to the cartilage surface, promoting the formation of a lubricating fluid film that separates surfaces and facilitates movement even during conditions of high opposing pressure and low articulating speeds.

The proposed lubricating mechanism depends solely on the structure of lubricin. So, analogous molecules with similar structures could potentially reduce boundary friction as well. This notion has inspired the use of synthetic polymer brushes as boundary lubricants bound to metal and mica surfaces [58]. It has also led to the modification of cartilage surfaces to bind viscous lubricants expanding their lubricating abilities and reducing boundary friction[62]. However, these methods involve forced tethering and the modification of cartilage surfaces and do not mimic the passive binding domain as part of the molecule that will allow for passive binding to the cartilage surface.

Thus, we hypothesized that biomimetic polymers with structures analogous to both the binding and lubricating domains of lubricin will be effectively bind to and lubricate articular cartilage. This study develops, tests, and tunes such synthetic lubricants and their efficacy at lubricating cartilage. To accomplish this, the objectives of this study were to (1) develop a library of tunable synthetic lubricants that mimic the lubricating and binding domains of lubricin; (2) characterize the ability of these lubricants to bind to cartilage surfaces through binding kinetics and dose response experiments; and (3) similarly characterize the ability of these polymers to lubricate cartilage.

3.3 Materials and Methods

3.3.1 Synthesis of Lubricin-mimetics: We mimicked the brush-like mucin domain by grafting hydrophilic polyethylene glycol (PEG) brushes to a polyacrylic acid (pAA) core. The pAA was synthesized via reversible addition−fragmentation chain-transfer polymerization (RAFT) polymerization using acrylic acid (AA), 4,4′-azobis 4-cyanopentanoic acid (A-CPA) and 4-cyanopentanoic acid dithiobenzoate (CPA-DB) under anhydrous, airtight and dark conditions [70]. In the reactions AA concentration was maintained (3 mM) while varying the concentrations of A-CPA and CPA-DB. A typical reaction scheme is as follows: AA (950 µl) was added to a flame dried 5 ml brown ampule with magnetic stirrer. Then CPA-DB (5.3 mg) was dissolved in nitrogen-purged methanol (2.9 ml) and added into the ampule. A-CPA (1.3 mg) was dissolved in of the nitrogen-purged methanol (0.7 ml) and added into the brown ampule mixture to initiate reaction. Nitrogen gas was run through the reaction mixture during and after the addition of each reagent for several minutes to prevent oxygen gas diffusion. After the last purging, the brown ampule was flamed sealed and placed in a 60^{o}C oil bath for 48 hours. Upon completion the ampule was broken, exposed to air and cooled in ice to stop further reaction. Next the solution was diluted and dialyzed against deionized water for 3 days then lyophilized to obtain a white, waxy powder.

PEG was then grafted to the pAA chain. The pAA-*graft*-PEG copolymer was synthesized via conjugation chemistry using 4-(4,6-Dimethoxy-1,3,5-triazin-2-yl)-4-methyl morpholinium chloride (DMTMM) as the coupling agent based on a procedure developed previously.[71] An example reaction is as follows: pAA (10 mg, M_W 107,600) and PEG-amine (0.151 g, M_W 2,000) were dissolved and mixed together in 2.4 ml of 0.1 M borate buffer (pH 8.5) in a 10 ml flask with stir bar. DMTMM (19.2 mg) dissolved in 0.6 ml of 0.1 M borate buffer was then added

drop-wise to the mixture and pH was adjusted to 6-7 using 1 M HCl. The reaction ran for 24 hours and then dialyzed against deionized water for 3 days, before being lyophilized to recover a white powder.

3.3.2 Bovine cartilage preparation. For the synthetic lubricants to mimic the boundary lubricating ability of lubricin, they must bind to the articulating surface. The thiol terminus of the pAA-*g*-PEG molecules was designed to interact with the collagen fibers of native cartilage. To evaluate the binding and lubricating ability of the lubricin-mimetics, we bound them to neonatal bovine cartilage. Full thickness bovine articular cartilage from the patellofemoral groove was removed at the chondro-osseus junction from 1-3 day old calves, and subsequently frozen at -20 degrees C. At the time of testing, the tissue was thawed in a water bath at 37 degrees C. A biopsy punch and a scalpel blade were used to form cartilage plugs 6 mm in diameter and 2 mm thick, keeping the superficial zone intact. Native lubricin was removed from the plugs by immersing them in a 1.5 M NaCl solution for 30 min, followed immediately by immersing them in PBS for 60 min.[74,53]

3.3.3 Attachment to cartilage & binding assessment. To evaluate polymer-cartilage binding, lubricin-mimetics were tagged with fluorescein-5-thiosemicarbazie via DMTMM chemistry in 0.1M borate buffer (pH 8.5) following a similar protocol to PEG conjugation onto pAA but without pH adjustment. The tagged polymer was dissolved in PBS and cartilage plugs were incubated in these solutions. Following the incubation, the plugs were rinsed twice with PBS to remove any unbound lubricants from the articular surface and then imaged.

Imaging was performed with a Zeiss 710 confocal microscope on a Zeiss Axio Observer Z1 inverted stand using a 40 /1.2 C-Apochromat water immersed objective operated by ZEN Software (Carl Zeiss MicroImaging, Jena, Germany). The cartilage surface was located by using

confocal reflectance and the fluorescently-tagged polymers were viewed using confocal fluorescence imaging. Confocal reflectance imaging was performed in conjunction with fluorescence imaging by splitting a 488nm laser. Confocal reflectance microscopy was performed at 475–510nm by collecting backscattered light reflected by collagen fibers through a 30μm pinhole and using a pixel dwell time of 1.58 μs. Fluorescently tagged lubricin-mimetics were captured at 500–580nm. In the images, red represents collagen content, while polymers are green. Once the surface was located by imaging the reflectance of the collagen fibers, the corresponding fluorescence image was used to indicate polymers at the cartilage surfaces. The fluorescence intensity was normalized to the collagen reflectance intensity to minimize topographical artifact (e.g. peaks or valleys that appear black on imaged surfaces).

3.3.4 Cartilage Lubrication. To assess the lubricating ability of the lubricin-mimetics, denuded cartilage plugs were incubated in solutions of the mimetics. After incubation, the plugs were rinsed twice with PBS to remove any unbound polymer from the tissue. The cartilage plugs were then loaded into our custom tribometer[78] to determine their frictional behavior. A 40% compressive normal strain was imposed on each cartilage plug, and 60 minutes was allowed for the hydrostatic pressure within the porous tissue to equilibrate.[75] The tribometer then linearly oscillated each plug against a polished glass counterface in a PBS solution at a speed of 0.3 mm/s. These conditions are well within boundary mode lubrication for this system.[75]

To assess binding kinetics, cartilage plugs for both binding assessment and friction testing were incubated in 3 mg/ml lubricin-mimetic solutions for incubation times of 0, 15, 30, 60, 90, and 120 min. Fluorescence intensity and friction data were plotted as functions of incubation time and were fit to first order binding models of the forms $Z = 1 - e^{(-t/\tau)}$ and $\mu = (\mu_\infty - \mu_0)\left(1 - e^{(-t/\tau)}\right) + \mu_0$, respectively where Z is the normalized fluorescence intensity, μ is

friction coefficient, μ_∞ is the coefficient of friction at maximal polymer binding, and μ_0 is the coefficient of friction in the absence of polymer binding. For dose response experiments, plugs were incubated for 120 min in lubricin-mimetic solutions of 0.03, 0.1, 0.3, 1, and 3 mg/ml. Similarly, the fluorescence intensity and friction data from the dose response experiments were plotted against lubricant concentration and fit to first order binding models of the form $Z = \frac{C}{K_D + C}$ and $\mu = (\mu_\infty - \mu_0)\left(\frac{C}{EC_{50}+C}\right) + \mu_0$, respectively where C is polymer concentration, K_D is the dissociation constant, and EC_{50} is the half-maximal effectiveness concentration.

3.3.5 Statistics. For the fitted parameters τ, K_D, and EC_{50}, a Monte Carlo analysis was used to simulate an n of 25 fits and the parameters were compared using a MANOVA. A MANOVA was used to compare the means of μ, τ, K_D, and EC_{50} between the polymer structural varialbles pAA size, PEG size, and PEG:AA density. Linear correlations were used to compare relationships between hydrodynamic size and the parameters μ, τ, K_D, and EC_{50}.

3.4 Results

3.4.1 Synthesis. A library of eight lubricin-mimetics was created with a range of backbone sizes, brush sizes, and brush densities. (Table 3.1) The modular design of the brush copolymers was aimed at creating a lubricin mimic with a tunable lubricating, mucin-like domain. The lubricating domain of the lubricin-mimetics was altered by controlling the three structural variables: pAA size, PEG size, and PEG density. Different lubricin-mimetics were synthesized using two sizes of the pAA backbones (60 and 105 kDa) and two sizes of the PEG side chains (2 and 10 kDa). Adjusting feed ratios during the conjugation process controlled brush density of each polymer configuration. PEG side chains were grafted on pAA backbones using different concentrations.

Table 3.1. Polymer Composition and Size

pAA Size (kDa)	PEG Size (kDa)	Feed Ratio (PEG:pAA)	Hydrodynamic Size (nm)
60	2	0.5	63
60	2	2	47
60	10	0.5	91
60	10	2	91
105	2	0.5	64
105	2	2	81
105	10	0.5	112
105	10	2	123

Feed ratios of 50 and 200-percent PEG-saturation were used, where a 100-percent feed ratio refers to grafting polymers in a solution supplying exactly enough PEG to fill every available slot on pAA backbones.

Changing the pAA backbone size, PEG brush size, and PEG brush density, enabled control of the hydrodynamic size of the lubricants. Hydrodynamic sizes of the polymers ranged from 46 to 123 nm, compared to 173 nm for lubricin[64], and 62 nm for the truncated lubricin mutant LUB:1[43,64]. Increasing the pAA size from 60 to 105 kDa increased hydrodynamic size in all polymers. Similarly, polymers with larger PEG side chains (10 kDa) had larger hydrodynamic sizes than those with smaller PEG chains (2 kDa). In fact, the hydrodynamic sizes of the lubricin-mimetics had the most dependence on PEG size, with the four largest polymer configurations containing the larger PEG side chains. The relationship between brush density and hydrodynamic size of the polymers was less clear. When the PEG:AA feed ratio was changed with regards to polymers with larger pAA backbones, an increase in the feed ratio from 0.5 to 2 uniformly resulted in polymers with larger hydrodynamic sizes. However, when this was done with regards to polymers with smaller pAA backbones, no such increase was observed.

3.4.2 Binding assessment. The lubricin-mimetics effectively bound to cartilage surfaces. (Figure 1) Cartilage surfaces were first located using the natural reflectance of the cartilage's collagen fibers. Then, fluoroscein-tagged polymers bound to the cartilage surfaces were imaged using fluorescence confocal microscopy. The lubricin-mimetics bound to the cartilage in a time dependent manner (Figure 3.1a-c). The polymers also had a specific affinity to collagen, evidenced by a higher local fluorescent intensity near the fibers (Figure 3.1c).

Time-dependent behavior of the binding of the lubricin-mimetics to cartilage was quantified using confocal intensity (Figure 3.2a). Binding for all the polymers fit well to first

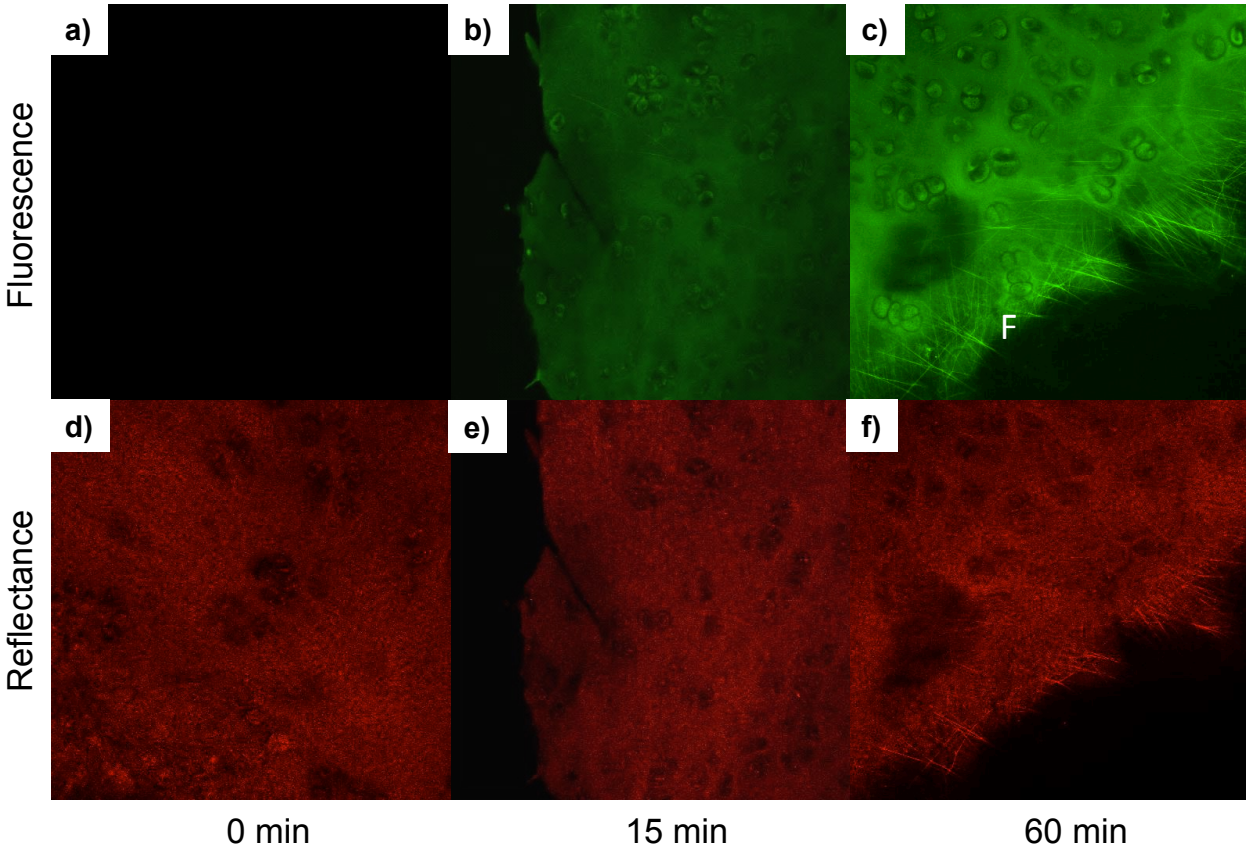

Figure 3.1. a-c) Fluorescence confocal microscopy shows binding of fluoroscein-tagged lubricin-mimetics to cartilage surfaces. **d-f)** The surface of cartilage was located using the natural reflectance of the collagen fibers of cartilage. The reflactance images remains at a relatively constant intensity. The fluorescent images above show an increase in fluorescent intensity as incubation time increases, indicating an increase in lubricant binding. Additionally, distinct fibers (F) have a relatively higher fluorescent intensity showing that the polymers have a specific affinity for collagen fibers.

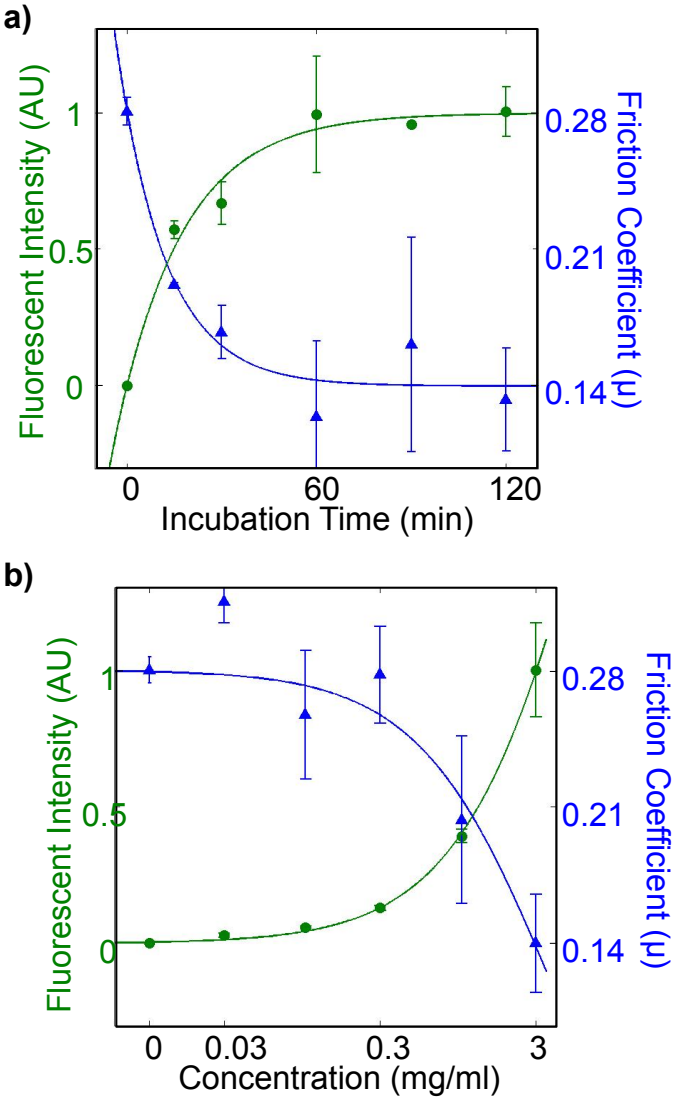

Figure 3.2. a) The biomimetic lubricants quickly bound to cartilage surfaces following first-order behavior (τ=20-41 min). Polymer lubrication was highly correlated with binding, with friction similarly decreasing as more lubricants attached to the surface (τ=20-39 min). **b)** Furthermore, the biomimetic lubricants exhibited dose-dependent behavior for both binding and lubrication. Polymer binding and lubrication were also highly correlated (r^2=0.89-0.98), with binding increasing and friction coefficients decreasing as polymer concentration increases. At 3 mg/ml, saturation points have yet to be reached. The estimated K_D and EC_{50}s are approximately 1-4 mg/ml.

order binding models (r^2=0.81-0.99; RMSE=0.053-0.14). Binding increased with incubation time, with time constants ranging from 20 to 39 minutes. Though these time constants are larger than those of lubricin (τ=8 min[41]), they are well below the clearance time of synovial fluid, approximately 5 hours, suggesting that the lubricin-mimetics would bind to the cartilage surfaces long before they leave the joint.

Similarly, lubricin-mimetics bound to cartilage in a dose dependent manner. (Figure 3.2b) Though we were unable to achieve saturation with our dose dependence experiments due to the limited solubility of the copolymer brushes at concentrations approaching 10 mg/ml, the data was fit to first order binding models (r^2=0.84-0.99; RMSE=0.0049-0.24). The range of the dissociation constants were K_D=0.5-3mg/ml, 1-3 orders of magnitude larger than the half maximal effectiveness constant of native full-length lubricin (EC_{50}=12μg/ml [41]).

3.4.3 Lubrication. Mimicking the mechanism of native lubricin, the bound lubricants effectively lubricated cartilage surfaces. The friction coefficients of all polymers behaved in a time dependent manner. Inversely to binding, friction decreased as incubation time increased. Friction coefficients fit well to first order binding models (r^2=0.76-0.99;RMSE=0.036-0.0.38), with time constants ranging from τ=20-41min. The ability of the lubricin-mimetics to bind to cartilage and their capacity to lubricate the tissue were highly correlated (r^2=0.89-0.99), with the binding behavior of the polymers closely resembling that of the frictional behavior.

Similarly, the lubricin-mimetics demonstrated a dose-dependent lubricating behavior, as friction coefficients decreased with an increase of polymer concentration. Again, due to limited solubility of the polymers approaching concentrations of 10mg/ml, friction coefficients tested may not have reached potential minima. The friction coefficients used were taken from samples that were incubated for 120min, anywhere from 3 to 6 times the lubricant-cartilage binding time

constants ensuring that polymer saturation had been reached on the cartilage surfaces at a given concentration. The data was fit to first order binding models (r^2=0.80-0.99; RMSE=0.069-0.25), with half maximal effective concentrations ranging EC_{50}=0.2-3mg/ml. These EC_{50} values correlated strongly (r^2=0.84-0.96) with the K_D values obtained from the dose response binding experiments, but are also 1-3 orders of magnitude larger than that of native full-length lubricin (0.19-4.1 mg/ml compared to 0.012 mg/ml for lubricin).

Like lubricin, the copolymer brushes effectively lubricated cartilage once bound. Six of the eight lubricin-mimetics tested significantly reduced friction coefficients, with coefficients of friction ranging from 0.140±0.024 to 0.248±0.030 compared to the coefficient of friction for cartilage stripped of lubricin μ_{eq}=0.276±0.007. (Figure 3.3) And while none achieved friction coefficients similar to that of lubricin (μ_{eq}=0.093±0.010 [41]), two of the eight had significantly lower friction coefficients than the truncated lubricin-mutant LUB:1 (μ_{eq}=0.23±0.02 [43]), which has previously demonstrated chondroprotective ability [43].

3.4.4 Structure-property relationships. The lubricin-mimetics were designed to have both tunable lubricating domains and tunable binding domains. The lubricating domain configuration is controlled by changing the structural variables pAA backbone size, PEG brush size, and PEG:AA brush density. By changing these variables, the physical characteristics of the polymer configurations varied significantly which is apparent in the range of hydrodynamic sizes previously discussed. As expected, changing the structural variables also affected the polymers' ability to bind to and lubricate cartilage.

While all lubricants bound relatively rapidly to cartilage surfaces, the binding time constants of the polymers depended on the composition and structure of the lubricin-mimetics. Increasing backbone size, side chain length, and feed ratio all significantly increased binding times ($p<0.05$;

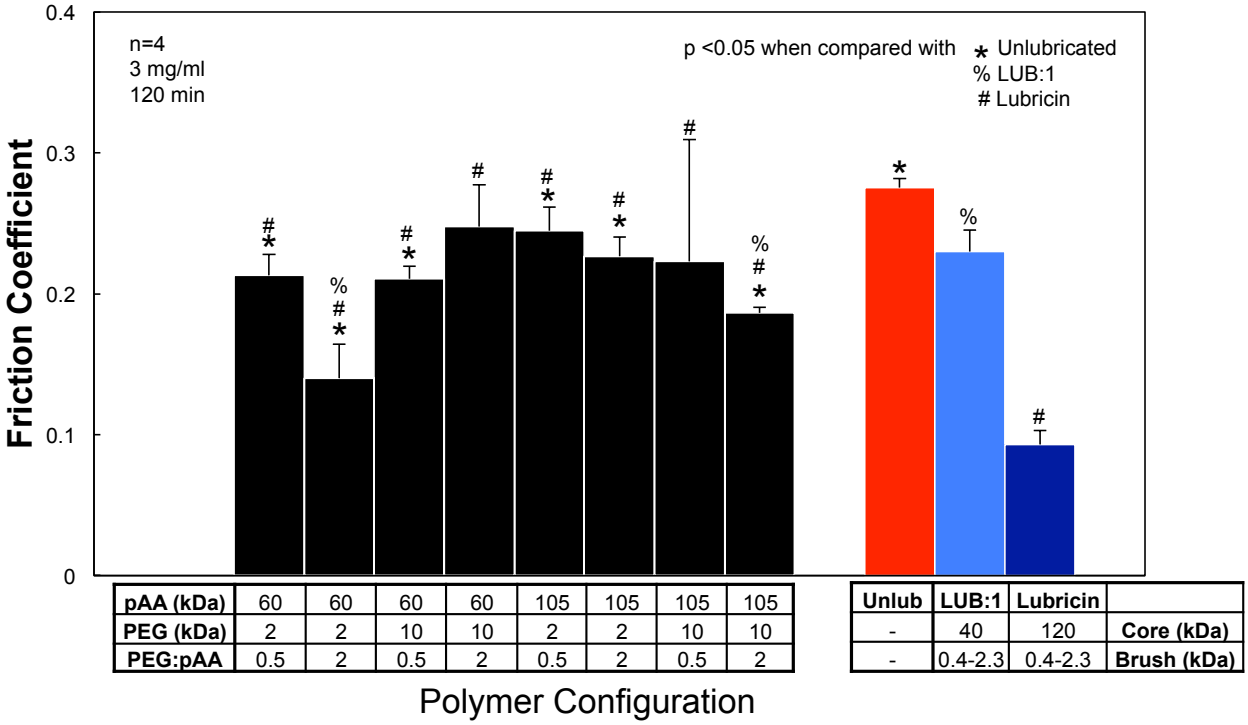

Figure 3.3. Like lubricin, the copolymer brushes effectively lubricated cartilage once bound. Six of the eight lubricin-mimetics tested significantly reduced friction coefficients compared to unlubricated cartilage (cartilage stripped of lubricin). And while none achieved friction coefficients similar to that of lubricin[75], three of the eight had significantly lower friction coefficients than the truncated lubricin-mutant LUB:1[43], which has previously demonstrated chondroprotective ability.

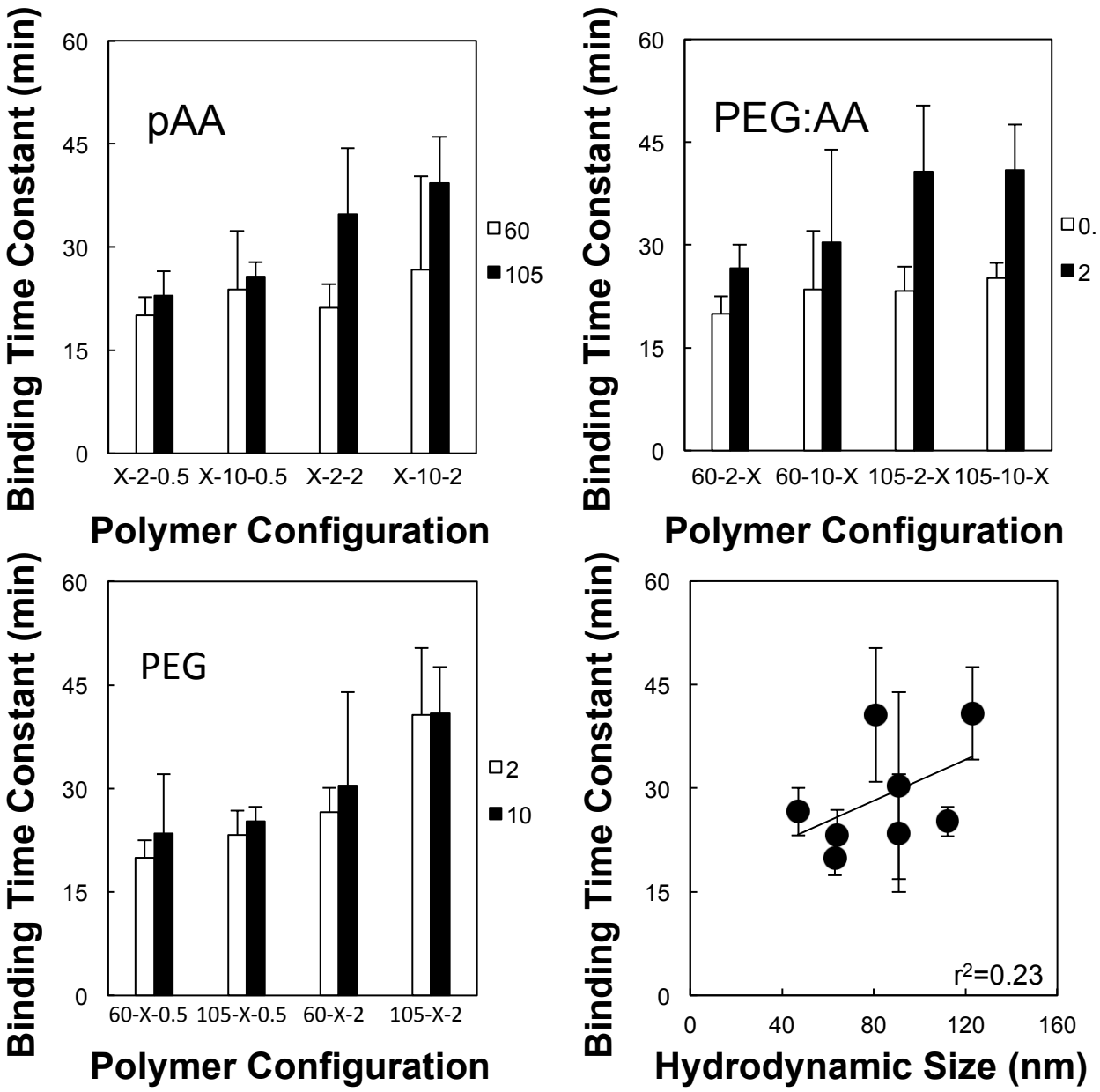

Figure 3.4. Polymer configurations with larger pAA backbone sizes ($p<0.01$), PEG side chain sizes ($p<0.05$), and PEG:AA grafting ratios ($p<0.01$) had larger binding time constants. Increasing both the pAA size and the PEG:AA feed ratio had a greater effect on lengthening binding times than did increasing either parameter alone ($p<0.01$), suggesting an interaction between the two structural parameters exists that influences binding.

Figure 3.4). Binding time constants were most sensitive to changes in PEG:AA feed ratios, increasing by an average of 50%. They were influenced by pAA backbone length (28% average increase) and PEG side chain length (10%) changes to a lesser extent. Furthermore, increasing both the pAA backbones and feed ratios lengthened binding times (64%, $p<0.01$) more than increasing either parameter alone, suggesting that an interaction between the two structural parameters influences binding.

The relationship between lubricant structure and lubricating ability was less clear. By changing pAA size, PEG size, and PEG brush density of the lubricin-mimetics, different coefficients of friction were observed. (Figure 3.5) A relationship with overall hydrodynamic size and friction coefficients was also undetermined. Two separate trends were observed between friction coefficients and hydrodynamic sizes of polymers with pAA backbone sizes 60 kDa and 105 kDa distinctly. Friction coefficients of polymers with pAA backbone sizes of 60 kDa increased as hydrodynamic size increased ($p<0.08$). Among those with 105 kDa pAA backbones however, polymers of larger hydrodynamic sizes lubricated more effectively ($p<0.05$).

3.5 Discussion

In this study, a family of biomimetic boundary lubricants was synthesized mimicking the brush-like structure of the natural glycoprotein lubricin and its ability to bind to and lubricate cartilage surfaces. With a thiol-terminated core, these lubricin-mimetics were able to adhere to the articular surface of cartilage, and because of this attachment they effectively lubricated the cartilage surfaces.

Much like lubricin, the lubricin-mimetics are boundary lubricants designed to self-assemble on cartilage sufaces, modifying and lubricating them. The copolymers are adsorbed on the

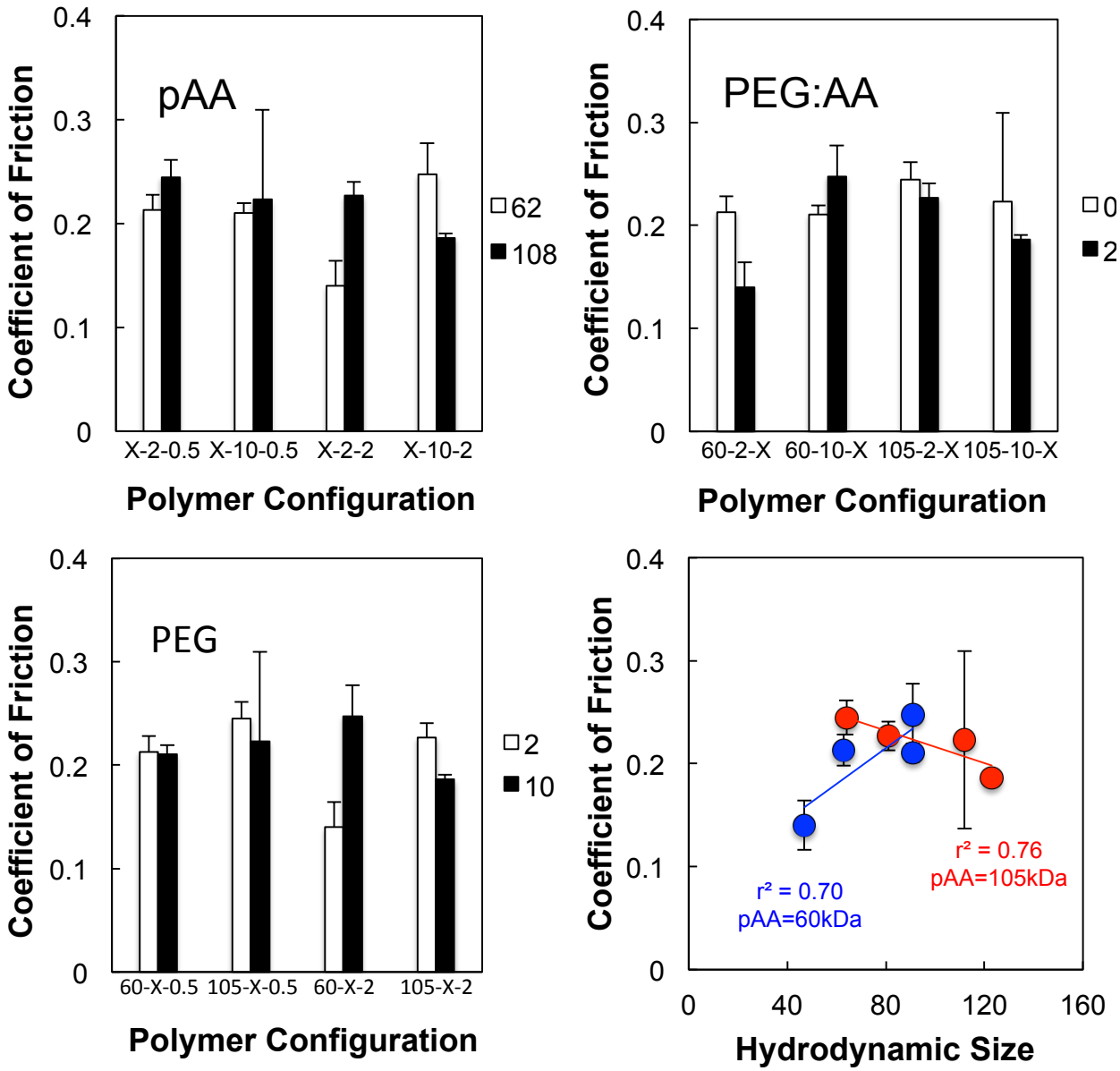

Figure 3.5. By changing the pAA size ($p<0.08$) and the PEG:AA density ($p<0.05$) of the lubricin-mimetics, different coefficients of friction were observed. Additionally, interaction terms existed between pAA size and PEG size ($p<0.01$), between PEG size and PEG:AA density ($p<0.05$), and between pAA size, PEG size, and PEG:AA density ($p<0.01$). However, the relationship between these structural variables and lubrication was unclear. A relationship with overall hydrodynamic size and friction coefficients was also undetermined. However, two separate trends are observed when looking at the relationship between friction coefficients and hydrodynamic sizes of polymers with pAA backbone sizes 60 kDa and 105 kDa distinctly. Friction coefficients of polymer configurations with pAA backbone sizes of 60 kDa increased with hydrodynamic size ($p<0.08$). Conversely, larger polymers with 105 kDa pAA backbones lubricated more effectively ($p<0.05$).

cartilage surfaces during incubation, creating a network of hydrophilic brushes across the articular surface that potentially traps a lubricating film. In these ways, both lubricin and the lubricin-mimetics exhibit behavior similar to a self-assembled monolayer (SAM). SAMs have been extensively studied to examine the adsorption of proteins and other biomolecules[72], and also at creating synthetic boundary lubricating films[65]. In SAMs, strong substrate binding and conformation of the brush structure greatly affect the lubricating properties.[67,60]

The high correlation between binding and lubrication shows that the lubrication mechanism of the lubricin-mimetics is strongly dependent on their ability to bind to the articulating surface. By binding to and modifying cartilage surfaces, these mucin-like polymers can act as boundary lubricants. In industrial applications, tribologists have looked to biology and to mucins to provide inspiration for finding effective boundary lubricants. Mucin-inspired copolymer SAMs have been developed to adhere to and lubricate metal bearings in systems within boundary friction.[58] In a similar vein, hyaluronic acid (HA) has been tethered to the cartilage surface to expand its lubricating abilities and effectively lubricate cartilage within boundary friction in vitro.[62] To our knowledge, this is the first report of synthetic lubricants inspired by and analogous to lubricin, the native boundary lubricant of the joint, that have successfully bound to and lowered boundary friction coefficients of cartilage.

The lubricin-mimetics bound rapidly to cartilage surfaces, exhibiting both time-dependent and dose-dependent behavior. The lubricating abilities of the polymers also exhibited both time and dose dependencies. The lubricating and binding behaviors of the synthetic lubricants closely paralleled each other with all time constants less than 40 min and both dissociation constants and half maximal effective concentrations on the order of 1 mg/ml. This underscores the therapeutic potential of these lubricating polymers, as they would bind to the collagen of cartilage surfaces in

synovial joints long before they would be cleared from the synovial fluid. Additionally, they would lubricate the cartilage at reasonable and soluble doses, facilitating their promising use as treatments for joint injury and disease.

Like native lubricin, the lubricin-mimetics exhibit dose-dependent lubricating behavior, but do so less efficiently that the native glycoprotein. The pAA-*g*-PEG copolymers bind through thiols, which bind to collagen throughout cartilage with an EC_{50} of 2.5 mM[79]. By contrast, the C-terminus of lubricin has affinity to both fibronectin and collagen[77,80], and binds to cartilage surfaces with an EC_{50} of 43 nM[53]. This discrepancy in binding efficiency could contribute to lubricin's superiority as a cartilage lubricant. To more closely mimic the C-terminus of lubricin and increase the lubricating abilities of the mimetics, the terminus of the polymers can be modified to enhance binding. Coupling the synthetics with a maleimide-PEG-NHS bifunctional group would allow the attachment of a more efficient peptide binding terminus. The peptide sequences TKKTLRT, SQNPVQP, and WYRGRL bind to collagen with IC_{50}s within the range of 100 to 300 nM [81,82]. Furthermore, WYRGRL has been used to bind nanoparticles to type-II collagen of cartilage tissue for potential therapeutic purposes [82], as well as acted as a tether for the attachment of other cartilage lubricants [62]. The peptide sequences VVEEDTTPQRPDVLVGGQSDPIDIDITEDTQPGMSGSNDAT[83] and VETEDTKEPGVLMG-GQSESVEFTKDTQTGMSGQTASQ[84] target fibronectin with EC_{50}s much less than 1μg/ml.

Binding times for the lubricin-mimetics increased with pAA backbone size, PEG side chain size, and PEG:AA side chain density ($p<0.05$). These data are consistent with trends observed with thiol-terminated polymer SAMs, where larger molecules took longer to assemble on surfaces[85]. The lubricin c-terminus consists of a 120-peptide sequence of approximately 20 kDa[53] and 2-3nm in length[68]. Increasing the size of the binding domain and the separation distance

from the dense brush of the mucin-like domain may facilitate binding. This larger domain with increased separation could be incorporated on the mimetics by adding a leader sequence. Through the use of the same maleimide-PEG-NHS bifunctional group, the inter-domain separation distance can be regulated. Simply increasing the size of the PEG molecule used in the bifunctional group would increase the separation distance and binding domain, and improve binding efficiency.

The lubricin-mimetics lubricated cartilage at concentrations of 3mg/ml, with six of the eight polymer configurations providing significantly lower boundary friction coefficients. Three of these polymer configurations had friction coefficients statistically similar to those the truncated lubricin mutant LUB:1, and the coefficients of the other three polymers were significantly lower. LUB:1 effectively lubricated cartilage and has shown chondroprotective ability[43]. The ability of lubricin and LUB:1 prevent cartilage damage is believed to be tied to the protective layer and lubricating film that they form when attached to the surface of cartilage[52,86]. In this case, the six synthetics that reduced friction levels have similar potential to prevent the progression of cartilage damage and degeneration, with three doing so more effectively than the mutant LUB:1. An in vivo study would determine which lubricin-mimetics protect synovial joints from degradation and provide insights on the chondroprotective mechanisms of lubricin. Furthermore, a relationship between chondroprotective ability and lubrication can be determined by testing a range of lubricin-mimetics that achieve different friction coefficients.

Two of the more researched lubricants of cartilage are lubricin and hyaluronic acid (HA). Lubricin's ability to operate as a boundary lubricant of cartilage is tied to its ability to attach to and hydrate the cartilage surface. Mucin-inspired synthetic boundary lubricants have been shown to lubricate mica and metal surfaces through similar mechanisms of binding and

hydrating[58,65,67,60]. Other polymers have been shown to effectively lubricate cartilage, but as viscous lubricants similar to hyaluronic acid and not as tethered boundary lubricants.[61] One group was able to tether the larger viscous lubricant HA to the cartilage surface to demonstrate boundary lubricating capacity, but did not mimic the passive binding domain that allows lubricin to self-assemble on cartilage surfaces[62]. To our knowledge, however, the pAA-*g*-PEG polymers presented in this study are the first known lubricin-mimetic, synthetic boundary lubricants on cartilage surfaces.

In this study, pAA-*g*-PEG copolymers effectively mimicked the structure and function of the cartilage lubricant lubricin. A library of eight polymers were synthesized with varying pAA backbone size, PEG side chain size, and PEG:AA side chain density. They bound to cartilage surfaces with binding time constants ranging from 20 to 41 min, and polymer binding was proportional to their lubricating ability. Six of the eight lubricin-mimetics effectively lubricated cartilage surfaces in vitro, with two mimetics lubricating more effectively than the lubricin-mutant LUB:1. Based on the chondroprotective ability of lubricin and LUB:1, these new materials may have promise as OA therapies.

4.0 Prevention of cartilage degeneration by intraarticular treatment with lubricin-mimetics

4.1 Abstract

Osteoarthritis is a leading cause of disability in the developed world that is initiated by mechanical damage to cartilage. This disease is characterized by dysregulation of lubricin, the primary boundary lubricant of cartilage located at the tissue surface and in synovial fluid. Recent work has demonstrated that supplementation of purified and recombinant forms of lubricin into the joint after injury can inhibit the onset and progression of arthritis in animal models of the disease. Here we report the synthesis of a polymer mimicking the structure and function of lubricin as a boundary lubricant and osteoarthritis therapeutic. The brush-like structure of lubricin was mimicked using biocompatible polymers composed of pAA and PEG. In vitro evaluation of binding to and lubrication of cartilage explants demonstrated effective binding times (< 40 mins) and significant reduction in friction compared to unlubricated controls ($p<0.001$). In vivo evaluation of pAA-*g*-PEG using a rat anterior cruciate ligament transection model showed significant reduction in friction compared to PBS controls and prevention of the formation of cartilage lesions and pathologic changes in subchondral bone (OARSI histology, $p<0.001$) suggesting potential as a OA therapeutic.

4.2 Introduction

Osteoarthritis (OA) is a leading cause of disability in adults caused by acute, chronic or progressive damage to the tissues surrounding joints such as the knees, hips or ankles[14]. In the United States, there were 27 million adults with OA in 2003[19] and this population is expected to grow to 67 million people by 2030[20]. In 2005, the annual health care burden of OA exceeded $185 billion[87] and the costs will continue to increase due to an aging population and increasing obesity rates.

Current pharmacologic treatments of OA include non-steroidal anti-inflammatories[21], intra-articular corticosteroid injections[22], and chondroitin sulfate or glucosamine supplements[23]; however, they have little or no effect on disease progression. A more recent approach to the treatment of OA involves the use of injectable lubricants to minimize friction and tissue damage. A common approach involves the intra-articular injection of the natural synovial glycosaminoglycan, hyaluronic acid (HA)[24], also known as HA viscosupplementation. HA increases synovial fluid viscosity, effectively altering lubrication mode toward mixed or hydrodynamic lubrication[10]. However, the mode of lubrication with the highest friction coefficients and incidence of wear is boundary lubrication, where opposing normal forces are high. Further, the efficacy of HA injections are a topic of continued debate, with studies showing only transient effects on pain relief that are minimally better than placebo and inconsistent evidence of benefit in radiographic assessment of disease progression.

More recently, there has been great interest in understanding the role of the natural synovial fluid glycoprotein, lubricin, in joint lubrication, Lubricin acts directly as a boundary lubricant by binding to the cartilage surface and appears to interact with HA to enhance cartilage lubrication in multiple lubrication modes.[45,88,89]. However, in damaged or aging cartilage, chondrocyte

production of lubricin is compromised and boundary mode lubrication is reduced[89]. Intra-articular injection of supplemental lubricin, as well as the truncated recombinant lubricin construct LUB:1, slows progression of OA in rat models of disease[43,45]. However, to date, the large-scale recombinant manufacture of both lubricin and LUB:1 remains challenging owing to multiple amino acid repeats in the protein core, as well as the high degree of glycosylation[56,90].

The potent boundary mode lubricating ability of lubricin stems from two key molecular features: its C-terminus and its central mucin domain. The C-terminus facilitates lubricin binding to fibronectin and collagen on the cartilage surface[52,56]. The mucin domain is a high-density oligosaccharide brush segment that attracts and retains water in a hydrogen-bonded network[52,91]. Collectively, these two molecular structures work in tandem to trap water proximally to the cartilage surface. The network of lubricin molecules across the articular surface of cartilage promotes the formation of a thin aqueous film to facilitate lubrication under boundary mode conditions[92].

Since lubricin's lubricating ability depends on its brush-like structure consisting of the aforementioned long mucin domain with hydrophilic side chains, our hypothesis is that lubricin is comparable to brush polymers in structure and function[52,91]. To this end, we aim to (1) synthesize brush polymers with analogous structures to lubricin will effectively bind to and lubricate cartilage surfaces, and (2) determine if molecules that bind to and lubricate cartilage surfaces will mitigate the progression of cartilage damage in vivo.

4.3 Materials & Methods

4.3.1 Materials. Acrylic acid (AA, 99.5%) stabilized with 200 ppm 4-methoxyphenol, methanol (99.8%) and sodium borate buffer were obtained from VWR (Radnor, PA, USA). 4,4'-azobis-(4-

cyanopentanoic acid) (A-CPA), Dulbecco's 10X Phosphate buffered saline (PBS), Sodium chloride (NaCl, >99.5%), 4-cyano-4-(phenylcarbonothioylthio)pentanoic acid (CPA-DB) (>97% HPLC) and fluorescein-5-thiosemicarbazie (~80%) was obtained from Sigma-Aldrich (St. Louis, MO, USA). Methoxy-poly(ethylene glycol)-amine powder (PEG-NH_2) was obtained from Jenkem Technologies (Beijing, PRC) and 4-(4,6-dimethoxy-1,3,5-triazin-2-yl)-4-methylmorpholinium chloride (DMTMM) was from TCI America (Portland, OR, USA). Knee joints of 1-3 day old calves were bought from butcher. All chemicals were used as received unless otherwise specified.

4.3.2 Synthesis and characterization of poly(acrylic acid) backbone (pAA). Polyacrylic acid was synthesized by RAFT polymerization using acrylic acid (AA), A-CPA as initiator (I) and CPA-DB as chain transfer agent (CTA) under anhydrous, airtight and dark conditions in methanol. AA concentration was maintained at ~3.8 mM, while [AA]:[I]:[CTA] was 762:0.25:1. The general reaction scheme is as follows: AA was added to a flame dried 5 ml brown ampule to which CPA-DB dissolved in 2.9 ml of nitrogen-purged methanol was added, followed by A-CPA dissolved in 0.7 ml of nitrogen-purged methanol. Nitrogen gas was bubbled through the reaction mixture to prevent oxygen influx. The ampule was flamed sealed and placed in a 60^oC oil bath for 48 hours. Ampule was then broken and cooled in ice bath. The solution was diluted with water, dialyzed against deionized water for 3 days, and then lyophilized to obtain a white, waxy powder. Characterization: ^1H NMR (INOVA 400 MHz, D_2O, ppm): δ1.5-2.0 (pAA-CH_2-), δ 2.25-2.75 (pAA-CH-). Molecular weight determined by Waters gel permeation chromatography (GPC) system (Waters 1515 Isocratic HPLC Pump, Waters 2414 Refractive Index Detector) using poly(methacrylic acid) standards and phosphate buffered saline (pH 7.4) as the mobile phase at 30^oC.

4.3.3 Synthesis of pAA-*g*-PEG polymer brushes. The pAA-*graft*-PEG (pAA-*g*-PEG) copolymer was synthesized by polymer analogous conjugation of monoamine-functionalized PEG to the pAA backbone using DMTMM as the coupling agent. pAA is dissolved in 0.1 M borate buffer (pH 8.5) at 3.3 mg/ml, while [AA]:[DMTMM]:[PEG] is 1:2:2. The general reaction is as follows: pAA and PEG-amine were dissolved in 3 ml borate buffer in a 10 ml flask with magnetic stir bar. DMTMM dissolved in in 0.6 ml borate buffer was added drop-wise into flask with the final pH adjusted to 6-7 using 1 N HCl. Each conjugation reaction was conducted for 24 hours at room temperature, dialyzed against deionized water for 3 days and lyophilized to obtain a white powder. Molecular weight was characterized by a multi-angle laser light scattering size exclusion chromatography (MALLS/SEC) performed at Biophysics Resource of Keck Facility at Yale University.

4.3.4 Bovine cartilage preparation & in vitro evaluation of pAA-*g*-PEG. For both kinetics and dose response experiments, cartilage plugs were taken from the patellofemoral groove of 1-3 day old bovine calves. Native lubricin was removed from the plugs using a 1.5 M NaCl solution. pAA-*g*-PEG were tagged with fluorescein-5-thiosemicarbazie via DMTMM chemistry in 0.1M Borate Buffer (pH 8.5) following a similar protocol to PEG conjugation onto pAA but without pH adjustment. The tagged polymer was dissolved in saline and cartilage plugs were incubated in these solutions. Following the incubation, the plugs were rinsed twice with saline to remove any unbound lubricants from the articular surface and then imaged with a Zeiss 710 confocal microscope.

In parallel, cartilage plugs denuded and incubated in solutions of pAA-*g*-PEG were loaded into our custom tribometer[56] to determine their frictional behavior. A 40% compressive normal strain was induced on each cartilage plug, and 60 minutes was allowed for the hydrostatic

pressure within the porous tissue to equilibrate. The tribometer then linearly oscillated each plug in a saline solution at a speed of 0.3 mm/s.

To assess binding kinetics, cartilage plugs were incubated in a 3mg/ml pAA-*g*-PEG solution for incubation times of 0, 15, 30, 60, 90, and 120 min. For dose response experiments, plugs were incubated for 120 min in lubricin-mimetic solutions of 0.03, 0.1, 0.3, 1, and 3 mg/ml.

Binding kinetics were assessed by measuring fluorescence intensity as a function of time and fitting this data to a first order binding model of the form $Z = A - Be^{(-t/\tau)}$.

4.3.5 Rat model of OA & in vivo evaluation of pAA-*g*-PEG. The pAA-*g*-PEG's were sterilized in 95% ethanol for ~0.5 hours and then dried, lyophilized and re-suspended in saline at 3 mg/ml. The anterior cruciate ligament (ACL) of each hind leg was transected in 11 Sprague-Dawley rats. Starting one week post-surgery, 50 µl of pAA-*g*-PEG solutions were injected intra-articularly into one knee, with the contralateral receiving a saline vehicle. The injections were repeated once per week for 3 weeks, and rats were sacrificed 3 weeks after the final injection. All animal studies were conducted in compliance with the Institutional Animal Care and Use Committee. Legs from six rats were examined histologically, while the other five were mechanically evaluated through tribometry and profilometry. Histologic samples were decalcified, embedded, sectioned, and stained with safranin-O. For mechanical evaluation, 3 mm cartilage samples were taken from the tibial plateau, one each from the medial and lateral compartments. Samples were loaded into a custom tribometer to determine their frictional behavior[56]. A compressive normal stress of 250-300 kPa was induced on each tibial plug and 60 minutes was allowed for the hydrostatic pressure within the tissues to equilibrate. The tribometer then linearly oscillated each explant in a saline solution at speeds of 0.1, 0.3, 1, 3, and 10 mm/s.

To observe roughening of cartilage, each tibial was then imaged on an ADE Phase Shift MicroXAM optical interferometric profiler and height measurements were taken over three different 849 μm x 631 μm scans. Histograms of the measured heights at each pixel of the scanned image were made. The deviations of these histograms are the surface roughness measure S_q.

4.4 Results

4.4.1 Polymer Synthesis & Characterization. To mimic the molecular composition and function of native lubricin, brush-like copolymers were designed and synthesized to impart both cartilage binding and hydrogen bonding domains. Specifically, polyethylene glycol (PEG) chains were grafted to a poly(acrylic acid) (pAA) core to mimic the central mucin domain of lubricin and the thiol terminus to allow binding to cartilage (**Figure 4.1a**). The synthesis of the lubricin mimetic was carried out using a robust, two-step synthesis. The pAA backbone was polymerized via RAFT polymerization of acrylic acid (AA) to produce a polymer M_n of 60,000 with a polydispersity of ~1.3 (**Figure 4.1b**). The pAA was conjugated with methoxy-PEG-amine (M_n 2,000) using DMTMM as the condensing agent (**Figure 4.1c**) with a final a M_n of $1.4*10^6$ with 80% degree of PEG substitution to the pAA backbone. Both of the polymer materials applied are biocompatible and are used extensively in the biomedical field.

4.4.2 Evaluation of in vitro treatments. To quantify the binding kinetics of pAA-*g*-PEG to cartilage, denuded bovine cartilage plugs were immersed in a solution of the polymer over various incubation times (**Figure 4.2a,b**). The pAA-*g*-PEG bound to the cartilage surfaces with a first order binding time constant of 16±1 min, reaching a maximum saturation after about 60(±2) min of incubation. Similarly, cartilage friction coefficients, measured under boundary

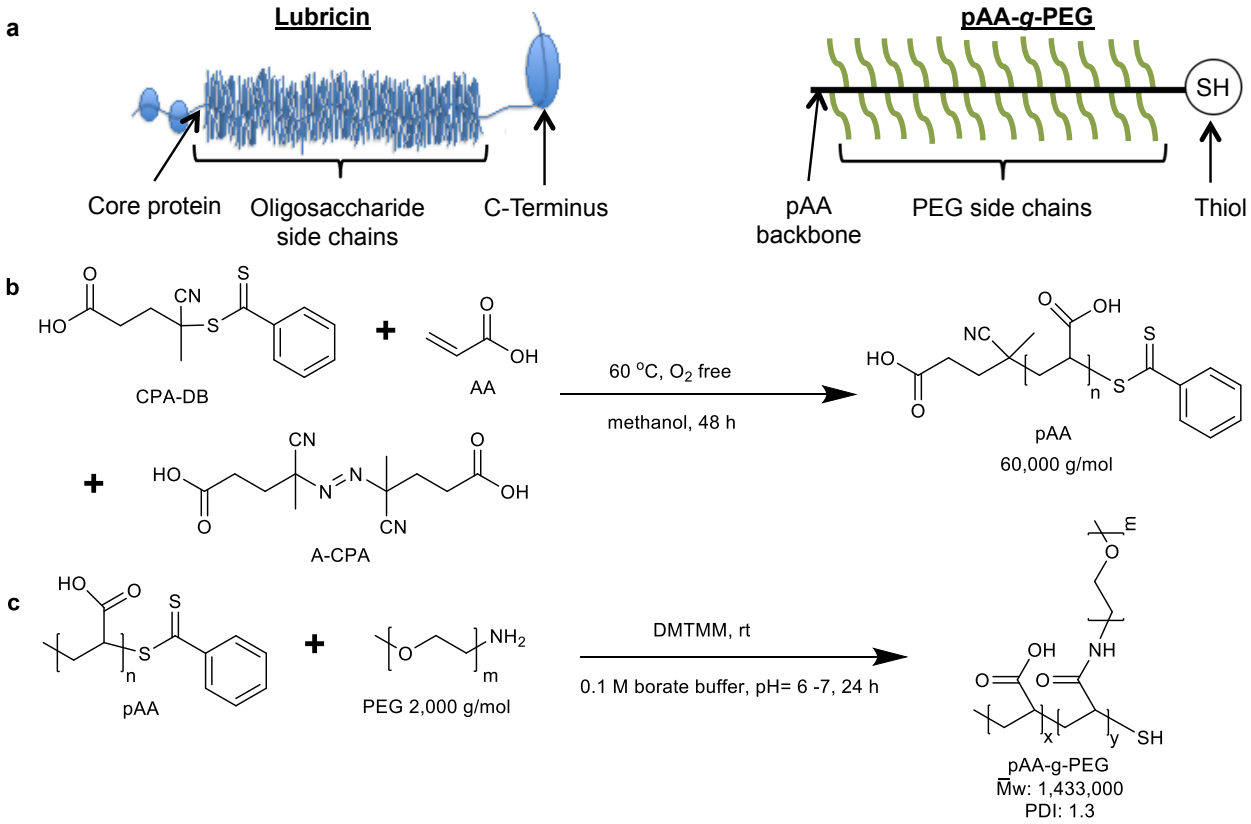

Figure 4.1. a) The design of pAA-*g*-PEG mimics the general structure of lubricin following the hypothesis that the lubrication properties is due to brush-like shape. In particular, the polymer pAA backbone, hydrophilic PEG side chains and thiol functional group mimics lubricin's core protein backbone, oligosaccharide chains and C-terminus respectively. **b)** Polymerization of acrylic acid(AA) CTA and initiator: 4-cyanopentanoic acid dithiobenzoate (CPA-DB), and 4,4′-Azobis(4-cyanopentanoic acid) (A-CPA) respectively. Molecular weight was determined done using aqueous SEC with poly(methacrylic acid) standards. **c)** Conjugation of 2,000 g/mol methoxy-PEG-amine to *60,000* pAA using activating agent 4-(4,6-dimethoxy-1,3,5-triazin-2-yl)-4-methylmorpholinium chloride (*DMTMM*) yielding a statistical graft copolymer called poly(acrylic acid)-*graft*-PEG or pAA-*g*-PEG. Aqueous MALLS/SEC was used to determine absolute molecular weight of pAA-*g*-PEG.

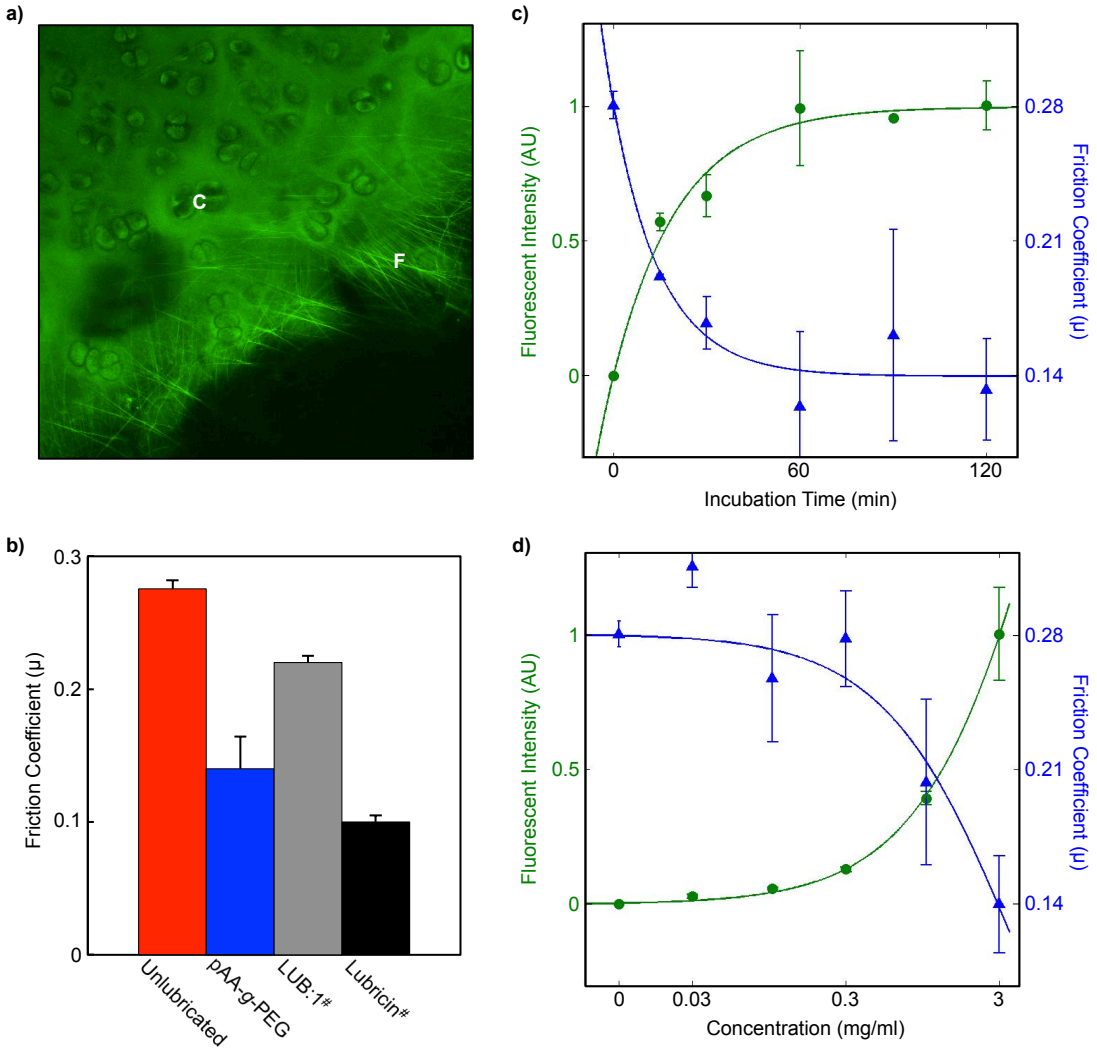

Figure 4.2. a) The image above shows fluorescently-tagged pAA-*g*-PEG (green) bound to cartilage surfaces. The polymers had particular affinity to collagen fibers near the cartilage surface, indicated by the bright green lines shown (F). A lack of binding was seen near the pericellular gaps surrounding the chondrocytes (C). **b)** The pAA-*g*-PEG effectively lubricated cartilage surfaces ($p<0.05$). Though it did not lubricate as effectively as lubricin[#], it lubricated better than the truncated lubricin mutant, LUB:1[#], which also exhibits chondroprotective behavior. **c)** The biomimetic lubricants quickly bound to cartilage surfaces following first-order behavior (τ=16 min). Polymer lubrication was highly correlated with binding, with friction decreasing as more lubricants attached to the surface also following first-order behavior with a comparable time constant (τ=20 min). These times are much shorter than the clearance times of synovial fluid (approximately 5 hrs[#]), indicating that the pAA-*g*-PEG will bind to cartilage surfaces long before being expelled from the joint. **d)** Furthermore, the biomimetic lubricants exhibited dose-dependent behavior for both binding and lubrication. Polymer binding and lubrication were also highly correlated ($r=0.98$), with binding increasing and friction coefficients decreasing as polymer concentration increases. At 3 mg/ml, saturation points have yet to be reached. The estimated K_D/EC_{50} is approximately 5mg/ml.

mode conditions, decreased as incubation time increased with a first order time constant of 20±1 min, reaching a minimum friction coefficient after about 60(±2) min of exposure. These are encouraging results, considering that the synovial clearance times for synovial fluid (about 5 hrs)[93] is an order of magnitude larger than the reported binding constants. So, injected pAA-*g*-PEG would bind to cartilage surfaces long before being expelled from the joint. Furthermore, overall friction coefficients decreased from μ=0.28±0.01 for denuded cartilage (cartilage surfaces without lubricin or pAA-*g*-PEG) to μ=0.14±0.02 for cartilage surfaces saturated with pAA-*g*-PEG demonstrating its efficacy as a boundary lubricant. As a comparison, the coefficient of friction for similar systems saturated with lubricin is about μ=0.10±0.01[41].

Dose response experiments were conducted using a constant incubation time while varying the lubricin-mimetic concentrations in which the cartilage plugs were incubated. The pAA-*g*-PEG both bound to and lubricated cartilage surfaces similarly to a first order binding model with a K_D and an EC_{50} = 1.3±__mg (10±1μM) (**Figure 4.2c**) The EC_{50} of lubricin is 11μg/ml[41]. Currently, saturation has not yet been observed for dosage suggesting a possible enhancement of lubrication at higher concentrations beyond those tested thus far.

We synthesized brush-like polymers with analogous structures to lubricin that rapidly bound to and effectively lubricated articular cartilage surfaces. Relatively low binding constants underscore the therapeutic potential of the pAA-*g*-PEG in that they may be able to bind to the cartilage surface well before being expelled from the joint. Additionally from these binding studies, lubrication was correlated with the amount of polymer bound to the surface (r=0.98), suggesting a dose-dependent effect for lubricant binding and function. Furthermore, the significant drop in friction for the pAA-*g*-PEG treated cartilage was comparable to that of lubricin and greater than that of the truncated lubricin mutant LUB:1 (**Figure 4.2d)**, both of

which have demonstrated chondroprotection in rat OA models[43,46]. Collectively, these results imply that pAA-*g*-PEG will effectively bind to and lubricate cartilage surfaces in vivo with potential chondroprotective results.

4.4.3 Mechanical and histological evaluation of in vivo treatment. The chondroprotective ability of the pAA-*g*-PEG was assessed using the widely-used anterior cruciate ligament transection (ACLT) model for OA in the rat knee[43–46,94]. The ACL of each hind leg of eleven Sprague-Dawley rats was transected. One limb of each rat was intraarticularly treated with a saline vehicle, while the contralateral received injections of a pAA-*g*-PEG solution. Plugs from the tibial plateaus of 6 of the rats were mechanically evaluated through friction testing and optical profilometry. Friction coefficients of the tibial plugs from the pAA-*g*-PEG-treated group were similar to those from healthy rats that had not undergone the ACLT procedure, and significantly lower than those from the saline-treated group (**Figure 4.3a**). The cartilage surfaces of the saline control group were significantly rougher than that of the lubricin-mimetic-treated group as well as the healthy group (**Figure 4.3b,c,d**). Thus, the pAA-*g*-PEG was able to preserve the lubricating ability and the morphology of the cartilage surface.

Histological grading was done for both the tibial and femoral surfaces of each joint of five rats using the OARSI scoring system[95] (**Figure 4.4**). No differences were seen in the scores of the tibial surfaces. However, in the femoral surfaces safranin-O staining of the histologic specimens revealed the presence of articular cartilage lesions, associated subchondral bone remodeling, evidence of significant proteoglycan loss, and focal regions of

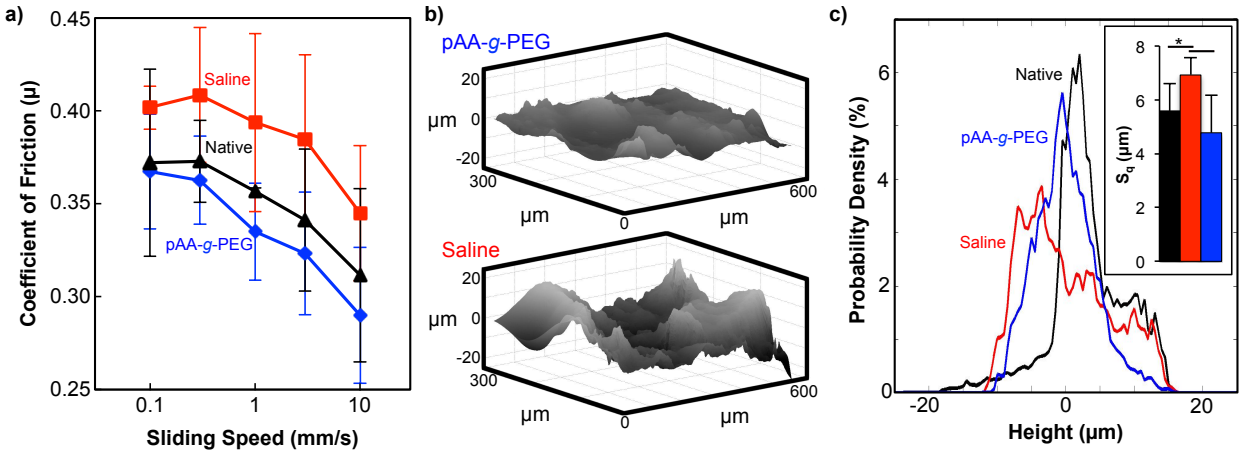

Figure 4.3. a) Intraarticular treatments with lubricin-mimetics preserved the low-friction bearing surface of the joint, evidenced by significantly lower friction coefficients for the polymer-treated group compared to saline-treated controls, $p<0.001$. The frictional behavior of the polymer-treated joints were similar to that seen in uninjured native joints. **b-c)** Intraarticular treatments with lubricin-mimetics also demonstrated chondroprotection by maintaining the smooth articular surface. Topographic images of the articular surfaces sample taken via optical profilometry showed narrower height distributions for polymer-treated cartilage compared to the saline-treated controls. The roughness of polymer-treated cartilage was similar to uninjured native surfaces.

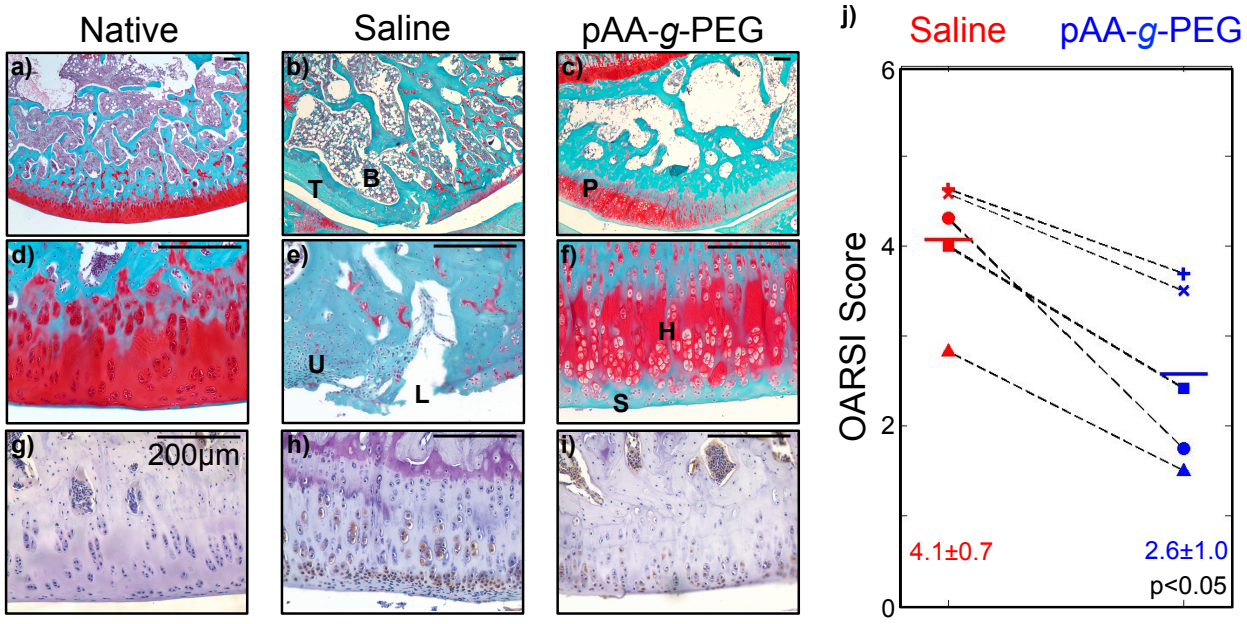

Figure 4.4. a-f) Chondroprotection by intraarticular treatments with lubricin-mimetics was evident in safranin-O stained histology. The polymer-treated joints showed better retention of proteoglycans (P) while maintaining a relatively intact and undisturbed articular surface (S). The saline-treated controls had large cartilage lesions (L), cartilage thinning (T) and morphologic subchondral bone changes (B), characteristic of advanced OA. Cells in the polymer-treated joints had healthy morphology and columnar arragement (H) similar to that in uninjured native joints. Cells in the saline-treated controls were unhealthy and near apoptotic (U). **g-i)** Caspase3 staining indicated much higher apoptotic cell presence in the untreated controls as compared to the native or the lubricin-mimetic treated joints. **j)** Chondroprotection by the lubrcin-mimetic treatments were quantified through OARSI scoring of each distal femur surface. The dashed lines shown connect the OARSI scores of the two femurs of a single rat. Lubricin-mimetic treatment prevented OA progression in each rat; the OARSI score of each pAA-*g*-PEG was lower than that of the corresponding saline-treated contralateral. The average OARSI score for polymer-treated femurs was about 2.5, corresponding to minimal surface disruption. The average score for the saline controls was approximately 4.0, signifying complete erosion of the cartilage surface and significant damage to the cartilage middle zone.

hypertrophy and cloning in the meniscus in the saline controls. In contrast, knees receiving injections of the pAA-*g*-PEG minimal changes in the articular surface, bone, or meniscus morphology and maintained healthy columnar cell arrangement throughout the cartilage. The OARSI score of each pAA-*g*-PEG-treated distal femur was lower than that of the contralateral. The mean score of the femoral surfaces of the saline control group was a 4.0, corresponding to the complete removal of the superficial zone of the cartilage as well as partial erosion of the middle zone. In contrast, the mean score for the femoral surfaces of the pAA-*g*-PEG-treated group was 2.5, corresponding to some disruption of the articular surface.

4.5 Discussion

The pAA-*g*-PEG copolymers prevented the progression of cartilage degeneration when introduced into ACL transected rat knees. Intraarticular injection of pAA-*g*-PEG prevented changes in cartilage, bone, and meniscus, functionally manifest in lower tissue roughness and friction coefficient. Notably the biggest cartilage changes were on the femoral condyles, yet roughening and changes in friction coefficient occurred on tibial cartilage.

Local administration of the pAA-*g*-PEG appeared to be therapeutically effective in preventing cartilage degeneration. The decrease in coefficients of friction for the pAA-*g*-PEG-treated group compared to the saline-treated group was $\Delta\mu=0.05$. Similar frictional changes have been seen between healthy and ACL-deficient joints as well as lubricin-deficient and wildtype rats ($\Delta\mu=0.03$[44] and 0.04[96], respectively). The introduced synthetic lubricants maintained levels of lubrication that have been previously observed in healthy, lubricin-rich joints. The lower friction coefficients in pAA-*g*-PEG-treated joints are consistent with the idea that cartilage degeneration is being mitigated, and the articular surface minimally disturbed. Such changes

changes in frictional behavior may be due to injected lubricants still bound to the cartilage or prevention of surface roughening and loss of endogenous lubricants.

The cartilage surfaces of the polymer treated group were smoother that those of the PBS treated group, having less variation in measured height across the surface. The relative smoothness is an indicator of preservation of cartilage health and also provides a lower friction bearing surface which will slow any degeneration through wear.

Furthermore, histologic analysis of rat knees treated with the pAA-*g*-PEG compare favorably to histologic results from similar studies using the truncated lubricin mutant LUB:1[43] and full length lubricin[44–47] at preventing the formations of cartilage lesions and hypertrophy. No gross damage to the articular cartilage or subchondral bone was observed in the histologic specimens for the polymer-treated group, which suggests that the pAA-*g*-PEG could be used as a potential therapy to treat degenerative diseases such as OA.

5.0 Boundary Lubricating Ability of Lubricin-mimetics as a Predictor of Chondroprotection

5.1 Abstract

In this study, the boundary lubricating ability of eight pAA-*g*-PEG brush co-polymers was measured by in vitro tribometry on bovine cartilage and used to predict their chondroprotective ability after intra-articular administration into ACL-deficient rat knees. These polymers mimic the structure and boundary lubricating function of lubricin, but not its biological activity. The lubricin-mimetics and were able to achieve a range of lubricating capacities by changing the structural parameters pAA backbone size, PEG brush size, and PEG:AA brush density. Six of the eight lubricants lowered boundary friction coefficients in vitro (μ=0.14±0.024 to 0.25±0.030; $p<0.05$). Two polymers were able to preserve lubricating properties ($p<0.05$) and prevent damage within the joint ($p<0.05$). A strong relationship was observed between the mimetics' boundary lubricating capacity and ability to prevent damage progression. Polymers that more effectively lubricated bovine cartilage in vitro both preserved the lubricating properties of cartilage surfaces (r^2=0.57; $p<0.05$) and prevented joint damage (r^2=0.51; $p<0.05$) in vivo.

5.2 Introduction

One of the primary functions of cartilage is to provide a low friction bearing surface that facilitates movement of synovial joints. In diseased or injured joints, friction is higher, which increases wear and accelerates damage progression.[55] The lubricating ability of cartilage has been linked to synovial fluid and its constituents. Specifically, the glycoprotein lubricin, found in synovial fluid and on the surface of cartilage[42], is the primary boundary lubricant of cartilage[40], reducing friction in conditions of high opposing forces and low articulating speeds. Furthermore, lubricin levels in osteoarthritic and damaged joints are lower[76], and the reintroduction of lubricin has shown the ability to mitigate the progression of cartilage degradation reducing damage by as much as 83 percent[43–49].

Recently a family of copolymer brushes was synthesized to mimic the structure and function of lubricin (Chapter 2). These molecules lubricated both model surfaces (Chapter 2) and cartilage (Chapter 3), with lubrication depending on polymer structure and conformation. Further, one such polymer was shown to protect cartilage from damage after ACL transection in vivo (Chapter 4). However, it remains unknown the extent to which the structure and properties of these polymers are related to their ability to protect cartilage.

While lubricin's chondroprotective properties are thought to arise from its action as a boundary lubricant, another proposed contributor to lubricin's chondroprotective ability is its biological activity within the joint. Both lubricin and LUB:1 affect joints biologically, including the ability to mediate cell adhesion [56] and the ability to bind and signal through CD44 receptors on chondrocytes and synoviocytes [57]. In contrast, there

have been no similar reports of biological activity from lubricin-mimetics. As such, the mechanism of chondroprotection by these boundary lubricants remains an open question. Previous work demonstrated that a family of biomimetic cartilage lubricants displayed a range of mechanical efficacy, lowering cartilage friction coefficients with $\Delta\mu$= -0.031 to -0.14. However, the ability of these lubricants to protect cartilage in vivo after joint injury is unknown.

Therefore, we hypothesized that the chondroprotective ability of these lubricin-mimetics depends on their lubricating capacity as measured in vitro. The specific goals of this study were to determine the relationships between the lubricating abilities of the lubricin-mimetics on cartilage surfaces in vitro and their abilities to (1) preserve low friction cartilage surfaces in injured joints intraarticularly treated with lubricin-mimetics in vivo, and (2) protect these joints from damage as measured by the Osteoarthritis Research Society International (OARSI) scoring system.

5.3 Materials and Methods

5.3.1 Synthesis. A library of eight pAA-*g*-PEG polymers was synthesized by methods described previously (Chapter 2). Two different sizes of the pAA core were synthesized: 105 kDa and 60 kDa. By grafting two different sized PEG chains (10 kDa and 2 kDa) to the pAA core and using two different PEG:AA feed ratios (2 and 0.5) for the conjugation chemistry, eight different polymers were created with varying backbone size, brush size, and brush density.

5.3.2 In vitro evaluation. The pAA-*g*-PEG copolymers were synthesized with a thiol terminus. This terminus was used to bind the polymers to collagen fibers of native

cartilage prior to friction testing (Chapter 3). Full thickness bovine articular cartilage from the patellofemoral groove was removed at the chondro-osseus junction of 1-3 day old calves, and subsequently frozen at -20 degrees C. At the time of testing, the tissue was thawed in a water bath at 37 degrees C. A biopsy punch and a scalpel blade were used to form cartilage plugs 6 mm in diameter and 2 mm thick, keeping the superficial zone intact. Native lubricin was removed from the plugs by immersing them in a 1.5 M NaCl solution for 30 min, followed immediately by immersing them in phosphate buffered saline (PBS) for 60 min.[53,74]

To assess the lubricating ability of the lubricin-mimetics, denuded cartilage plugs were incubated in solutions of the mimetics. After incubation, the plugs were rinsed twice with PBS to remove any unbound polymer from the tissue. The cartilage plugs were then loaded into our custom tribometer[78] to determine their frictional behavior. A 40% compressive normal strain was imposed on each cartilage plug, and 60 minutes was allowed for the hydrostatic pressure within the porous tissue to equilibrate.[75] The tribometer then linearly oscillated each plug against a polished glass counterface in a PBS solution at a speed of 0.3 mm/s. These conditions are well within boundary mode lubrication for this system.[75]

5.3.3 In vivo evaluation. The chondroprotective ability of the eight lubricin-mimetics was evaluated using a post-traumatic OA model in rats as previously described (Chapter 4). All animal studies were conducted in compliance with the Institutional Animal Care and Use Committee of the Hospital for Special Surgery. For this study, 95 Sprague-Dawley rats were separated into eight different treatment groups with 12 rats in each of seven groups and 11 rats in one group. The rats in each of the eight groups were treated

with a different lubricin-mimetic solution. Eight different lubricin-mimetic solutions were prepared. The lubricin-mimetics were sterilized in 95% ethanol for 0.5 hours and then dried, lyophilized and re-suspended in PBS at 3 mg/ml.

For the injury model, the anterior cruciate ligament (ACL) of each hind leg was transected in each rat. Starting one week post-surgery, each rat received an intra-articular injection of 50 μl of the respective lubricin-mimetic solution into one knee, and a 50-μl injection of a PBS vehicle into the contralateral. The selection of which knee received treatment and which knee received vehicle (i.e. right or left) was randomized. The injections were repeated once per week for 3 weeks, and rats were sacrificed 3 weeks after the final injection.

Legs from six rats from each group were examined histologically, while the other six were mechanically evaluated through tribometry and profilometry. Histologic samples were decalcified, embedded, sectioned, and stained with safranin-O. Two independent graders trained in using the Osteoarthritis Research Society International (OARSI) scoring system[95] graded each histology slide, quantifying any cartilage damage seen within the joint. The graders were blinded as to which slides belonged to treated or untreated limibs and also to which group.

For mechanical evaluation, cartilage samples 3 mm in diameter were taken from the tibial plateau, one each from the medial and lateral compartments. Samples were loaded into a custom tribometer[78] to determine their frictional behavior. A compressive normal stress of 250-300 kPa was induced on each tibial plug and 60 minutes was allowed for the hydrostatic pressure within the tissues to equilibrate[75]. The tribometer then linearly oscillated each explant in a PBS solution at a speed of 0.3 mm/s, outputting the shear

load. The friction coefficients were determined from the ratios of the shear to normal loads.

5.4 Results

5.4.1 In vitro evaluation. Six of the eight lubricin-mimetics significantly reduced boundary friction coefficients of neonatal bovine cartilage, with coefficients of friction ranging from μ=0.14±0.024 to 0.25±0.030 compared to the coefficient of friction for cartilage stripped of lubricin μ=0.28±0.007. (Figure 5.1) And while none achieved friction coefficients similar to that of lubricin (μ=0.093±0.010 [41]), two of the eight had significantly lower friction coefficients than the truncated lubricin-mutant LUB:1 (μ=0.23±0.02 [43]), which has previously demonstrated chondroprotective ability[43].The two lubricin mimetics with coefficients of friction lower than LUB:1 were pAA(105)-2-PEG(10) (μ=0.19±0.004) and pAA(60)-2-PEG(2) (μ=0.14±0.024).

5.4.2 In vivo treatment. A wide spectrum of cartilage damage was observed across the treatment groups. Examining tissue from the untreated controls, representative samples of the femoral surfaces appeared to be more damaged than the tibial surfaces. The femurs from joints receiving PBS injection exhibited large articular cartilage lesions and had evidence of surface erosion, cartilage thinning, and associated subchondral bone remodeling. (Figure 5.2) In these samples, little to no safranin-O staining was observed indicating a significant loss of proteoglycan content within the cartilage and focal regions of hypertrophy and cloning were present in the menisci. Additionally, the cell morphology was markedly unhealthy and disorganized with large numbers appearing apoptotic. In contrast, the untreated tibiae displayed minimal surface disruption with

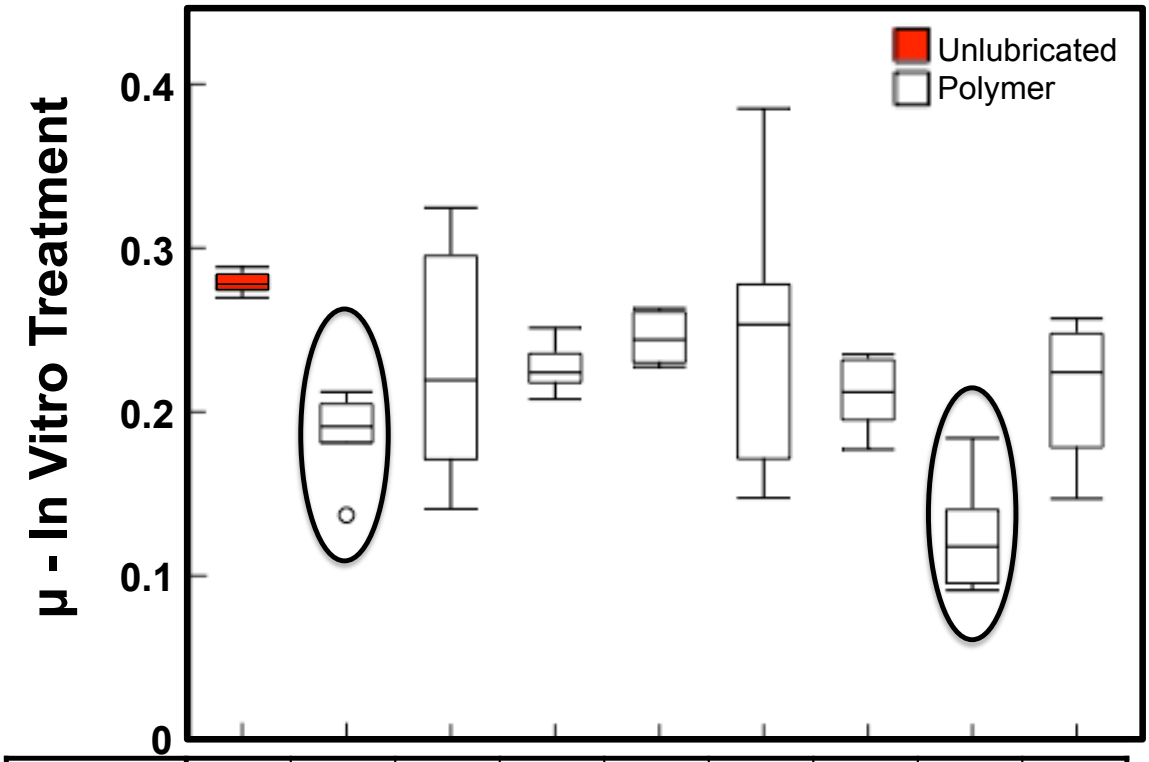

pAA (kDa)	-	105	105	105	105	60	60	60	60
PEG (kDa)	-	10	10	2	2	10	10	2	2
PEG:AA	-	2	0.5	2	0.5	2	0.5	2	0.5

Figure 5.1. A boxplot of the friction coefficients of neonatal bovine cartilage with bound lubricin-mimetics is show. Six of the eight polymers effective lubricated cartilage surfaces compared tho the friction coefficients of unlubricated tissue. The pAA(105)-*g(2)*-PEG(10) and The pAA(60)-*g(2)*-PEG(2) significantly reduced friction compared to unlubricated.

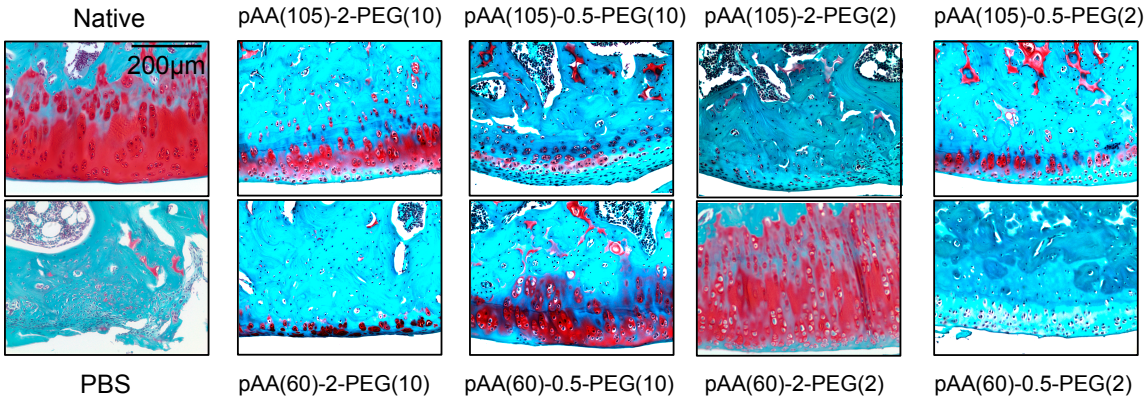

Figure 5.2. Representative histology slides are shown for each lubricin-mimetic treatment as well as both positive and negative controls.

relatively intact middle to deep zone cartilage (images not shown). This data suggests that within the ACL transection model of the Sprague-Dawley rat, OA progression acts more rapidly and aggressively on the distal femur than the tibial plateau.

Across the eight different lubricin-mimetic treated groups, a wider range of effects was seen. Several groups displayed similar damage to what was seen in the untreated femurs, most notably tissue taken from femurs treated by the lubricin-mimetics pAA(105)-2-PEG(10) and pAA(60)-0.5-PEG(10). The samples that most resembled native cartilage came from femurs treated with pAA(60)-2-PEG(2). The tissue from these joints displayed minimal changes to the articular surfaces, bone, or meniscus morphology and maintained healthy columnar cell arrangement throughout the cartilage.

Quantification of the observed joint degradation was done using the OARSI scoring system. Histological grading was done for both the tibial and femoral surfaces of each joint of each rat. The tibial surfaces were significantly less damaged than the femoral surfaces for all groups and all treatments ($p<0.01$), with OARSI scores of 2.9. As a result, no differences were seen between the scores of the treated or untreated tibial surfaces. However, the distal femur appeared more susceptible to damage and degradation following ACL injury in the rat, providing some insight of the progression of OA within the joint in this injury model.

Comparing the OARSI scores of the femoral surfaces of each group provided a better indication of how the lubricin-mimetics affected joint degradation. (Figure 5.3) The treated femurs from two of the eight groups, pAA(105)-0.5-PEG(10) and pAA(60)-2-PEG(2), had significantly lower OARSI scores when compared to the untreated contralaterals ($p<0.05$). The median score of the pAA(105)-0.5-PEG(10)-treated femoral

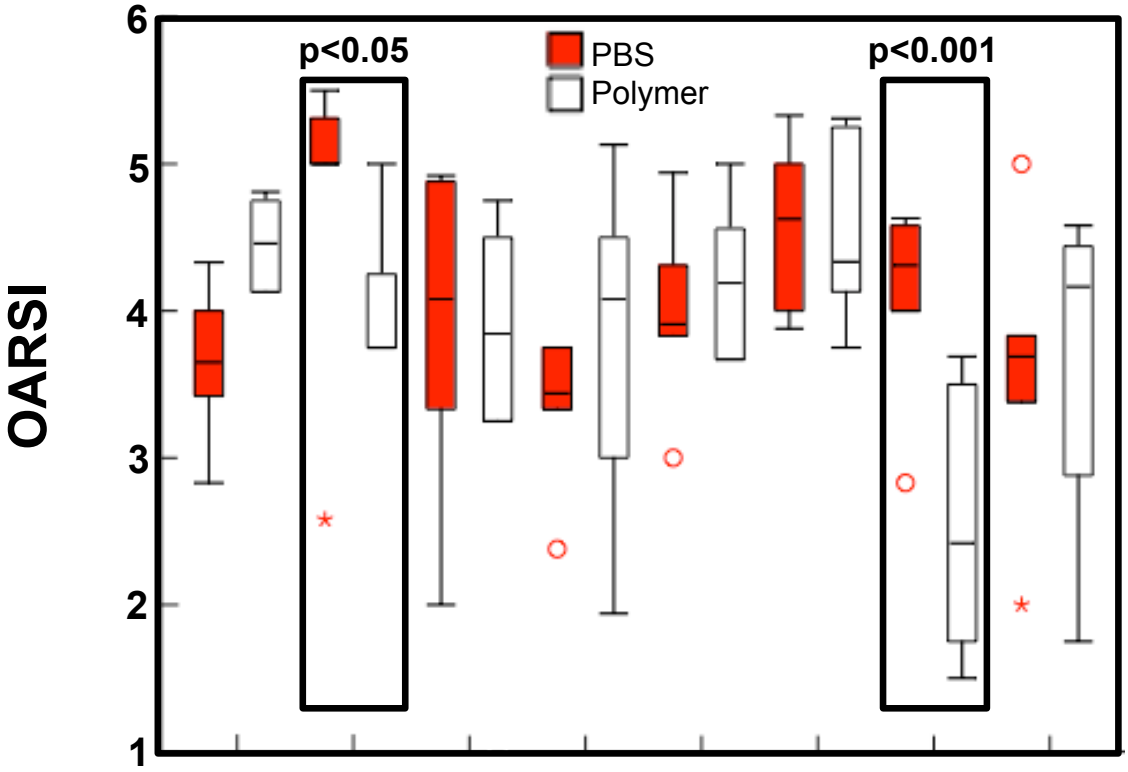

pAA (kDa)	105	105	105	105	60	60	60	60
PEG (kDa)	10	10	2	2	10	10	2	2
PEG:AA	2	0.5	2	0.5	2	0.5	2	0.5

Figure 5.3. Histology was quantified using the OARSI scale. The pAA(105)-*g(0.5)*-PEG(10) and The pAA(60)-*g(2)*-PEG(2) were significantly lower than their PBS-treated contralaterals.

surfaces was 3.8, corresponding to significant superficial zone damage and some middle zone dame of the cartilage. In contrast, the median score of the untreated contralateral femurs within this group was 5.0, corresponding to total superficial zone erosion, severe middle and deep zone damage, and signs of delamination of the cartilage from the tidemark.

Within the group of rats treated with pAA(60)-2-PEG(2), the range of cartilage damage and corresponding OARSI scores were much different. The median scores of the pAA(60)-2-PEG(2)-treated femurs was 2.4, corresponding to some disruption of the articular surface within an otherwise healthy joint. The median of the contralateral control group was a 4.3, corresponding to the complete removal of the superficial zone of the cartilage as well as partial erosion of the middle zone.

Much like the cartilage treated in vitro, the lubricin-mimetics had a range of efficacy at maintaining the lubricating properties of cartilage when treated in vivo. (Figure 5.4) Joint surfaces treated with pAA(105)-0.5-PEG(10) and pAA(60)-2-PEG(2) maintained lower friction coefficients than the untreated contralaterals ($p<0.05$). The two lubricin-mimetics that best preserved lubricating properties are the same two that demonstrated the ability to preserve joint integrity in the histological analysis and OARSI grading, strongly suggesting a relationship between healthy cartilage structure and lubricating function.

5.4.3 In vitro-in vivo relationships. Polymers that lubricated bovine cartilage more effectively in vitro demonstrated greater chondroprotective ability in vivo. The lubricin-mimetics prevented cartilage and joint damage in injured rat knees with varying efficacy, with the chondroprotective ability of each mimetic was predicted by in vitro tribometry.

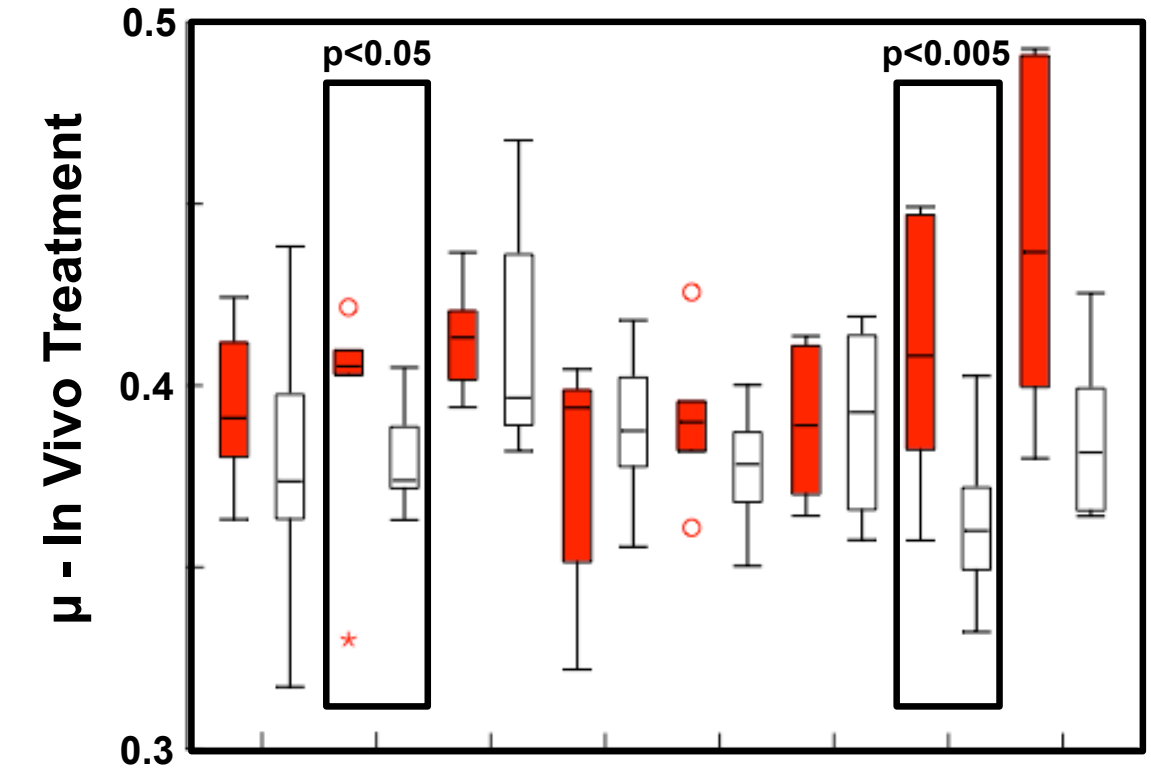

pAA (kDa)	105	105	105	105	60	60	60	60
PEG (kDa)	10	10	2	2	10	10	2	2
PEG:AA	2	0.5	2	0.5	2	0.5	2	0.5

Figure 5.4. Friction coefficients for the treated and control rat joints are shown. The pAA(105)-*g(0.5)*-PEG(10) and The pAA(60)-*g(2)*-PEG(2) were significantly lower than their PBS-treated contralaterals.

OARSI score was significantly correlated (r^2=0.51, $p<0.05$) with friction coefficient measured in vitro on neonatal bovine cartilage. (Figure 5.5a) These data indicate that higher friction in this model system was predictive of damage in vivo after ACL transection.

Similarly, polymers that lubricated bovine cartilage explants in vitro preserved the lubricating abilities of rat cartilage surfaces when injected into the joints of rats after ACL transection. While a relationship between the structure of the molecules and their lubricating abilities was not determined, the lubricating ability of the lubricin-mimetics translated from in vitro experiments to in vivo environments. The friction coefficients of rat cartilage treated in vivo was significantly correlated (r^2=0.57, $p<0.05$) with the friction coefficients of bovine cartilage tested in vitro. (Figure 5.5b)

5.5 Discussion

In this study, a library of synthetic lubricin-mimetics displayed the ability to lubricate and protect cartilage to varying degrees, and their chondroprotective ability was predicted using in vitro tribometry. Six of the eight lubricin-mimetics effectively lubricated neonatal bovine cartilage in vitro. Lubricants most effective at lowering boundary friction coefficients in vitro were also most effective at protecting cartilage from damage and preserving lubricating properties of cartilage in vivo after joint injury.

Friction coefficients for bovine cartilage tested with lubricin-mimetics in vitro correlated with friction coefficients for cartilage treated in vivo with the lubricin-mimetics after traumatic injury (r^2=0.57) and with their OARSI scores (r^2=0.51). These correlations indicate that the primary mechanism behind the chondroprotective effect of

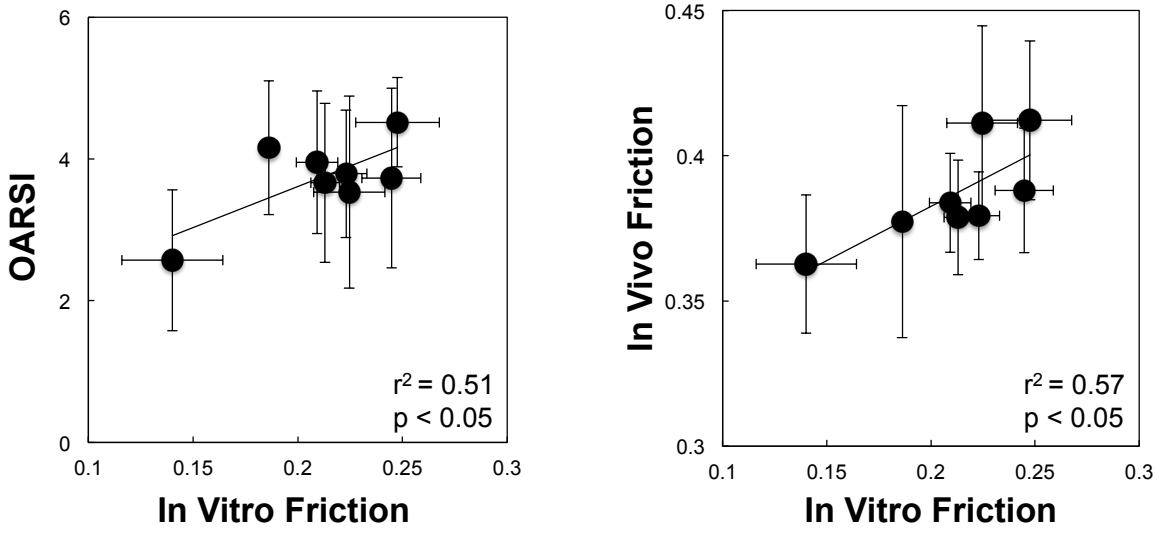

Figure 5.5. Friction coefficients and OARSI grades for the in vivo treated rat joints and were significantly correlated with in vitro friction testing of the polymers on neonatal bovine cartilage

the lubricin-mimetics is their lubricating ability. However, these findings do not rule out the existence of chondroprotective biological effects by lubricin. The strengths of the correlations are not high enough to declare boundary lubricating ability as the sole mechanism of chondroprotection, but they are large enough to indicate that the boundary lubricating ability of such lubricants is the predominant predictor for preserved healthy cartilage morphology.

The decrease boundary friction coefficients for the pAA(60)-2-PEG(2)-treated tibiae compared to the untreated contralaterals was $\Delta\mu$=-0.04. Similar frictional changes have been seen in whole joint friction tests between healthy and ACL-deficient joints as well as lubricin-deficient and wildtype rats ($\Delta\mu$=-0.03[44] and -0.04[96], respectively). While multiple tissues and structures may contribute to whole joint friction, these similarities in changes in boundary friction coefficients suggest that cartilage-cartilage friction plays a particularly important role. The introduced synthetic lubricants maintained levels of lubrication that have been previously observed in healthy, lubricin-rich joints. By contrast, pAA(105)-0.5-PEG(10) seemed to prevent moderate OA from becoming severe and decreased friction coefficients by $\Delta\mu$=-0.02. The discrepancy in OARSI score coupled with the differences in lubricating ability between the two effective lubricin-mimetics bolsters the link between lubrication and chondroprotection.

Notably the biggest morphological changes in the joint were observed on the femoral condyles, yet changes in friction coefficient occurred on tibial cartilage. This provides some insight regarding the progression of OA in the rat knee, as the femoral surfaces seemed to be affected by damage more rapidly and aggressively. One limitation that stems from this phenomenon is that the friction experiments could only be done with

explants taken from the tibial plateau. The curvature of the femoral condylar surfaces in the rat prevents sufficient contact to obtain reliable coefficients of friction using a linearly oscillating tribometer[75].

To better mimic in vivo conditions, other tribological studies used rotational cartilage-on-cartilage[61,63,96] or pendulum-based ex vivo[47,96–99] systems. In this study, boundary lubricating ability was tested in vitro on a linearly oscillating, cartilage-on-glass tribometer using neonatal bovine explants under physiologically low normal loads[75]. This system does not mimic the natural conditions of the joint, yet still predicted the chondroprotective efficacies of the lubricin-mimetics. It remains unknown whether the use of murine cartilage or cartilage-on-cartilage systems would provide stronger predictive ability.

Furthermore, this study predicts the chondroprotective ability of known boundary lubricants. It is unclear if this approach could be extended to predict the efficacy of hyaluronic acid[100] or untethered synthetic macromolecules[61] that function more as viscous lubricants, because within the boundary lubricating regime of this system, viscous lubricants show no effect on friction coefficients[40].

Multiple studies have shown lubricin's ability to protect cartilage.[43–46] However, it remains unknown whether this chondroprotective mechanism is mechanically or biologically driven. The lack of lubricin within a joint leads to joint surfaces of reduced lubricating capacities as well as cartilage viability[96]. The degree of chondrocyte apoptosis was correlated with cartilage-cartilage friction coefficients. These data suggest that lubricin's lubricating ability plays an important role in chondroprotection, but stops short of demonstrating a connection between the degree of lubrication and the degree of

protection. Here, the boundary lubricating ability of synthetic lubricants predicted the extent to which they prevent damage, supporting the idea that boundary lubricants can protect joints by mechanical mechanisms.

6.0 Conclusion

Lubricin is a potent boundary lubricant of articular cartilage that has shown the ability to prevent the progression of cartilage damage in joints. These two properties of the glycoprotein are believed to be linked. Specifically, the proposed mechanism behind this chondroprotection is boundary lubrication. Additionally, the mechanism behind lubricin's lubricating ability is linked to two key structures: a cartilage binding domain and a mucin-like lubricating domain. The studies presented here explore the lubricating and chondroprotective abilities of synthetic boundary lubricants modeled after lubricin.

This dissertation presents investigations developing a family of eight biomimetic boundary lubricants with analogous structures to the glycoprotein lubricin as effective treatments for cartilage injury. Chapter 2 examined the effects of changing the structural parameters of the synthetic lubricants affected the way in which they modified idealized surfaces and lubricated cartilage. Chapter 3 characterized the binding of the polymers to cartilage surfaces, and their lubricating efficacy once bound. Chapter 4 detailed the chondroprotective role of the lubricants when introduced in vivo. And Chapter 5 explored the link between the in vitro lubricating ability and the in vivo chondroprotective ability of the lubricin-mimetics, developing the basis of a potential cartilage injury and disease therapy screening process.

Chapter 2 characterized how the lubricin-mimetics adsorbed to and modified gold-coated surfaces and how that affected cartilage friction. The most significant outcome of this chapter was that the lubricin-mimetics effectively lubricated cartilage. Additionally, changing the structural parameters of the lubricating domains of the lubricin-mimetics was shown to alter the molecule's hydrodynamic size, their lubricating ability, and the

characteristics of the modified surface. A correlation was observed where friction coefficients decreased as the hydrodynamic size of the lubricant increased. This structure-function relationship is reinforced by the comparable size and lubricating abilities of the chondroprotective LUB:1.

In Chapter 3, the lubricin-mimetics were bound directly to cartilage surfaces. The lubricants rapidly bound to cartilage, bolstering their potential for use in vivo as they would bind to cartilage before being expelled from the joint. Six different lubricants also effectively reduced the boundary friction coefficients cartilage once bound. Lubricating ability and binding were highly correlated, showing the dependence of the lubricating mechanism on lubricant binding. This is consistent with the lubricating mechanism of lubricin, where the C-terminus achors the protein to the cartilage surface to allow for boundary lubrication.

The study in Chapter 4 demonstrated that a lubricin-mimetic, pAA(60)-2-PEG(2) prevents cartilage damage and lowers the cartilage coefficient of friction in an in vivo model of cartilage injury. The results show that the introduction of the synthetic boundary lubricant following mechanical injury in vivo prevents damage and the increase in boundary friction that would otherwise occur. This study develops the relationship between boundary lubrication and chondroprotection. The lubricin-mimetics were designed as boundary lubricants of cartilage, and were effective. In doing so, they maintained a relatively smooth cartilage surface and low OARSI scores indicating chondroprotection. This suggests that boundary lubrication plays a major role in preventing cartilage damage progression.

In Chapter 5, the coefficients of friction for cartilage treated with the lubricin-mimetics in vitro were correlated to both the OARSI scores and friction coefficients of injured joints treated with the lubricants in vivo. This relationship shows the primary mechanism for chondroprotection in joints to be boundary lubrication. Additionally, the boundary lubricating abilities of boundary lubricants can be used as a predictor as to how well they will lubricate and preserve joint tissue in diseased or injured joins. This predictor can be used to screen potential therapies, ruling out less promising treatments prior to having gone through extensive and exhaustive animal studies.

The major contributions of this work are two fold: 1) a mechanistic understanding of how cartilage damage progression and boundary lubrication are linked, and 2) the development of supplemental boundary lubricants that have the potential to treat cartilage injury and disease. The examination of cartilage boundary lubrication focused on understanding the structural mechanisms by which lubricin is able to effectively lubricate cartilage in boundary mode and using that understanding to develop synthetic analogues to lubricin as a means to treat joint injury and disease. Chapters 2, 3, and 5 explored the dependence of lubricating ability on the structural parameters of the synthetic lubricating domain. Like many boundary lubricants, the lubricin-mimetics adsorbed to and modified an articulating surface. The mimetics were able to bind to and modify idealized gold surfaces (Chapter 2), cartilage surfaces in vitro (Chapter 3), and cartilage surfaces in vivo (Chapters 4 and 5), lubricating them as a result. Though no relationship between the structural parameters and lubricating ability was found, tuning the mucin-like domain of the lubricants provided different levels of lubrication. Furthermore, the efficacy of the binding domain was crucial for proper lubrication by the lubricin-mimetics. Dictated by

the two functional domains, this boundary lubricating ability of the lubricants was able to preserve cartilage tissue and function while preventing cartilage damage progression to a similar degree seen by lubricin. Lubricants chemically disparate but structurally similar to lubricin showed similar abilities to protect cartilage from damage, confirming that the two functional domains of lubricin provide its lubricating activity and demonstrating that the chondroprotective action in joints is largely governed by both lubricin and the ability to effectively reduce boundary friction. Moreover, the lubricating activity of cartilage boundary lubricants in vitro is a direct correlate to their ability to prevent joint damage and degradation (Chapter 5).

The synthetic boundary lubricants provide insights on the mechanism of how lubricin lubricates and protects cartilage, establishing their therapeutic potential. Mechanical injury causes a host of changes in the joint, including the depletion of of lubricin from the cartilage surface.[45] Lubricin injected in such injured or damaged joints has slowed damage progression[43–49] to a degree similarly seen by the injections of certain lubricin-mimetics. By mimicking the structures of lubricin, the lubricin-mimetics were able to bind to, lubricate, and protect cartilage. The lubricin-mimetics show strong potential to be developed as cartilage injury therapies, and the library of different lubricin-mimetics linked lubricating ability with chondroprotection establishing the basis for the development of a screening process to more easily and efficiently evaluate such therapies.

6.1 Study Limitations & Future Directions

Efforts to characterize how the lubricin-mimetics interacted with the articulating surface did not translate from the gold-coated glass slides to cartilage. And while fluorescent microscopy provided information about the rates of binding and saturation on the cartilage surfaces, the relative amounts of lubricants binding to the surface were undetermined. To better understand how the lubricants modify articulating surface, the cartilage surface could be analyzed directly. Fourier transform infrared spectroscopy (FTIR) has been used to characterize the composition of both pAA- and PEG-based polymers[101] and cartilage[102]. Linear combinations of the spectra for the lubricin-mimetics and the cartilage surface can be found to match the spectra for cartilage surfaces with bound lubricants. This process would quantify the amount of lubricants being absorbed. Additionally, specific ECM components such as collagen or fibronectin could be physisorbed onto a surface to allow for similar FTIR image decomposition to determine the interaction of the lubricin-mimetics to each component. This would also allow for an additional method to evaluate the effect of tuning the binding domains of the lubricin-mimetics.

The dose response experiments did not achieve saturation of lubricin-mimetic binding, and the estimated half-maximal effectiveness concentrations were approximately 2 orders of magnitude larger than that of lubricin[43]. Increasing the efficiency of the binding of the lubricin-mimetics will increase the efficiency of lubrication with the same lubricity levels achieved by smaller doses, and potentially will increase lubrication through the use of concentrations where the maximal effectiveness occurs. To achieve these ends, collagen or fibronectin binding peptide sequences[81–84] with dissociation

constants on the order of that of lubricin could be attached to the thiol terminus of the lubricin-mimetics allowing for more efficient binding to the surface.

Furthermore, the in vitro tribology experiments evaluate friction in a controlled environment that is not representative of the complex architecture of the joint. Specifically, the comparisons to lubricin and evaluation of the lubricin-mimetics ignore the interactions ignore interactions with other snovial fluid constituents. Lubricin has exhibited synergistic tribological effects when paired with hyaluronic acid (HA) in particular[88]. HA-binding peptide sequences have been identified[103], and can be used in conjunction with the lubricin-mimetics to allow the tethering of HA to the surface expanding the lubricating scope of the molecules.

The in vivo experiments were done in Sprague-Dawley rats. To further develop the molecules as potential treatments, toxicology and large animal studies must be completed. Acute, subacute, and subchronic systemic toxicity in male Lewis rats consist of subcutaneous injections for experimental durations of 6 months, and will provide foundational data for long-term biological effects. During these experiments, the lubricin-mimetics could also be fluorescently-tagged and their residence times in the joint tracked. Additionally, long-term efficacy trials using a Pond-Nuki (ACLT) model for OA in dogs for durations of 7, 14, and 21 weeks will illuminate the long-term chondroprotective ability of the synthetic lubricins. While pAA[104] and PEG[105] have been used for medical applications before, these studies will better evaluate the copolymers' biological effect in vivo. Beyond these developmental steps, better understanding the polymers' role in vivo would add to the mechanistic understanding of how they function. A similar FTIR decomposition as described above can be performed to see how much polymer is being

adsorbed in vivo. Additionally, tagging the lubricants with a fluorescent dye and tracking their residence times within the joint will lead to better clinical development understanding when they need to be replenished leading to the development of potential treatment regimens.

Another limitation of the in vivo study presented in this work is the limited progression of tibial damage seen. Mechanical evaluation found differences in the behavior of the tibial surfaces, but the range of those differences would potentially be expanded if a wider spread of cartilage damage were evident similar to that seen for the femoral surfaces. The curvature of the femoral surfaces prevents their use for mechanical testing. Extending the time frame of the in vivo trial or alternatively using a more aggressive destabilized medial meniscal transection[43] model of OA would provide such a wider range of joint damage. Extending the range of damage for mechanical evaluation would also provide better resolution for analyzing the link between in vitro lubrication and in vivo chondroprotection enhancing a treatment screening process development.

In summary, synthetic polymers that mimic the structure of lubricin effectively bound to, lubricated, and protected cartilage. The development of these lubricin-mimetics elucidated the boundary lubrication mechanisms of lubricin behind its chondroprotectve ability. The lubricin-mimetics showed strong potential for therapeutic development, with one lubricant able to protect cartilage similarly to its parent protein. Increasing the binding efficiencies of the polymers and extending the current studies to include toxicology and large animal trials should be the next stages of development.

REFERENCES

(1) Lu, X. L.; Mow, V. C. *Med. Sci. Sports Exerc.* **2008**, *40*, 193–199.

(2) Hascall, V.; Kimura, J. *Methods Enzymol.* **1982**, *82*, 769–800.

(3) Eyre, D. *Arthritis Res.* **2002**, *4*, 30–35.

(4) Eyre, D. R.; Pietka, T.; Weis, M. A.; Wu, J.-J. *J. Biol. Chem.* **2004**, *279*, 2568–2574.

(5) Poole, A. R.; Kojima, T.; Yasuda, T.; Mwale, F.; Kobayashi, M.; Laverty, S. *Clin. Orthop. Relat. Res.* **2001**, S26–S33.

(6) Grodzinsky, A.; Levenston, M. *Annu. Rev. ...* **2000**, 691–713.

(7) Mow, V. C.; Kuei, S. C.; Lai, W. M.; Armstrong, C. G. **2013**, *102*, 73–84.

(8) Forster, H.; Fisher, J. **1996**.

(9) Buschmann, M.; Grodzinsky, A. *J. Biomech. Eng.* **1995**, *117*, 179–192.

(10) Eisenberg, S.; Grodzinsky, A. *J. Orthop. Res.* **1985**, *3*, 148–159.

(11) McCutchen, C. *Wear* **1962**, *5*.

(12) Krishnan, R. *J. Orthop. ...* **2004**, *22*, 565–570.

(13) Simon, W. *J. Biomech.* **1971**, *4*, 379–389.

(14) Guccione, A. *Am. J. Public Health* **1994**, *84*, 351–358.

(15) Bland, J. H.; Cooper, S. M. *Semin. Arthritis Rheum.* **1984**, *14*, 106–133.

(16) Martin, J.; Buckwalter, J. *Biogerontology* **2002**, *3*, 257–264.

(17) Martin, J. *J. Orthop. ...* **1997**, *15*, 491–498.

(18) Buckwalter, J. a; Brown, T. D. *Clin. Orthop. Relat. Res.* **2004**, *423*, 7–16.

(19) Lawrence, R. C.; Felson, D. T.; Helmick, C. G.; Arnold, L. M.; Choi, H.; Deyo, R. a; Gabriel, S.; Hirsch, R.; Hochberg, M. C.; Hunder, G. G.; Jordan, J. M.; Katz, J. N.; Kremers, H. M.; Wolfe, F. *Arthritis Rheum.* **2008**, *58*, 26–35.

(20) Hootman, J. M.; Helmick, C. G. *Arthritis Rheum.* **2006**, *54*, 226–229.

(21) Scott, D. L.; Berry, H.; Capell, H.; Coppock, J.; Daymond, T.; Doyle, D. V; Fernandes, L.; Hazleman, B.; Hunter, J.; Huskisson, E. C.; Jawad, a; Jubb, R.; Kennedy, T.; McGill, P.; Nichol, F.; Palit, J.; Webley, M.; Woolf, a; Wotjulewski, J. *Rheumatology (Oxford)*. **2000**, *39*, 1095–1101.

(22) Arroll, B.; Goodyear-Smith, F. *BMJ* **2004**, *328*, 869.

(23) Sinusas, K. *Am. Fam. Physician* **2012**, *85*, 49–56.

(24) Mabuchi, K.; Tsukamoto, Y.; Obara, T.; Yamaguchi, T. *J. Biomed. Mater. Res.* **1994**, *28*, 865–870.

(25) Swann, D. a; Radin, E. L.; Nazimiec, M.; Weisser, P. a; Curran, N.; Lewinnek, G. *Ann. Rheum. Dis.* **1974**, *33*, 318–326.

(26) Bannuru, R. R.; Natov, N. S.; Dasi, U. R.; Schmid, C. H.; McAlindon, T. E. *Osteoarthritis Cartilage* **2011**, *19*, 611–619.

(27) Chang, K.-V.; Hsiao, M.-Y.; Chen, W.-S.; Wang, T.-G.; Chien, K.-L. *Arch. Phys. Med. Rehabil.* **2013**, *94*, 951–960.

(28) JUBB, R. W.; PIVA, S.; BEINAT, L.; DACRE, J.; GISHEN, P. *Int. J. Clin. Pract. 57*, 467–474.

(29) Hersey, M. D. *J. Washingt. Acad. Sci.* **1914**, *4*, 542–552.

(30) Shaw, M. C.; Nussdoerfer, T. J. **1947**.

(31) Cudworth, C. J.; Higginson, G. R. *Wear* **1976**, *37*, 299–312.

(32) Philipossian, A.; Olsen, S. *Jpn. J. Appl. Phys.* **2003**, *42*, 6371–6379.

(33) Pitenis, A.; Urueña, J.; Schulze, K. *Soft Matter* **2014**, *10*, 8955–8962.

(34) Szeri, A. Z. *Fluid film lubrication: theory and design.*; Cambridge University Press, 1998.

(35) Dowson, D. *History of Tribology*; Longman London, 1979.

(36) Murti, P. *Wear* **1971**, *18*, 449–460.

(37) Stewart, T.; Jin, Z. M.; Fisher, J. *211*, 451–465.

(38) Aviad, A. D.; Houpt, J. B. *J. Rheumatol.* **1994**, *21*, 297–301.

(39) Dahl, L. B.; Dahl, I. M.; Engstrom-Laurent, A.; Granath, K. *Ann. Rheum. Dis.* **1985**, *44*, 817–822.

(40) Jay, G. D.; Haberstroh, K.; Cha, C. J. *J. Biomed. Mater. Res.* **1998**, *40*, 414–418.

(41) Gleghorn, J. P.; Jones, A. R. C.; Flannery, C. R.; Bonassar, L. J. *J. Orthop. Res.* **2009**, *27*, 771–777.

(42) Swann, D. a; Sotman, S.; Dixon, M.; Brooks, C. *Biochem. J.* **1977**, *161*, 473–485.

(43) Flannery, C. R.; Zollner, R.; Corcoran, C.; Jones, A. R.; Root, A.; Rivera-Bermúdez, M. a; Blanchet, T.; Gleghorn, J. P.; Bonassar, L. J.; Bendele, A. M.; Morris, E. a; Glasson, S. S. *Arthritis Rheum.* **2009**, *60*, 840–847.

(44) Teeple, E.; Elsaid, K. a; Jay, G. D.; Zhang, L.; Badger, G. J.; Akelman, M.; Bliss, T. F.; Fleming, B. C. *Am. J. Sports Med.* **2011**, *39*, 164–172.

(45) Jay, G. D.; Fleming, B. C.; Watkins, B. a; McHugh, K. a; Anderson, S. C.; Zhang, L. X.; Teeple, E.; Waller, K. a; Elsaid, K. a. *Arthritis Rheum.* **2010**, *62*, 2382–2391.

(46) Jay, G. D.; Elsaid, K. a; Kelly, K. a; Anderson, S. C.; Zhang, L.; Teeple, E.; Waller, K.; Fleming, B. C. *Arthritis Rheum.* **2012**, *64*, 1162–1171.

(47) Teeple, E.; Elsaid, K. A.; Fleming, B. C.; Jay, G. D.; Aslani, K.; Crisco, J. J.; Mechrefe, A. P. *J. Orthop. Res.* **2008**, 231–237.

(48) Vugmeyster, Y.; Wang, Q.; Xu, X.; Harrold, J.; Daugusta, D.; Li, J.; Zollner, R.; Flannery, C. R.; Rivera-Bermúdez, M. a. *AAPS J.* **2012**, *14*, 97–104.

(49) Elsaid, K. a; Zhang, L.; Waller, K.; Tofte, J.; Teeple, E.; Fleming, B. C.; Jay, G. D. *Osteoarthritis Cartilage* **2012**, *20*, 940–948.

(50) Jay, G. D.; Harris, D. a; Cha, C. J. *Glycoconj. J.* **2001**, *18*, 807–815.

(51) Flannery, C. R.; Hughes, C. E.; Schumacher, B. L.; Tudor, D.; Aydelotte, M. B.; Kuettner, K. E.; Caterson, B. *Biochem. Biophys. Res. Commun.* **1999**, *254*, 535–541.

(52) Coles, J. M.; Chang, D. P.; Zauscher, S. *Curr. Opin. Colloid Interface Sci.* **2010**, *15*, 406–416.

(53) Jones, A. R. C.; Gleghorn, J. P.; Hughes, C. E.; Fitz, L. J.; Zollner, R.; Wainwright, S. D.; Caterson, B.; Morris, E. A.; Bonassar, L. J.; Flannery, C. R. *J. Orthop. Res.* **2007**, *12*, 10–12.

(54) Zappone, B.; Greene, G. W.; Oroudjev, E.; Jay, G. D.; Israelachvili, J. N. *Langmuir* **2008**, *24*, 1495–1508.

(55) Jay, G. D.; Torres, J. R.; Rhee, D. K.; Helminen, H. J.; Hytinnen, M. M.; Cha, C. J.; Elsaid, K.; Kim, K. S.; Cui, Y.; Warman, M. L. *Arthritis Rheum.* **2007**, *56*, 3662–3669.

(56) Jones, A.; Gleghorn, J. *J. Orthop. Res.* **2007**, *12*, 10–12.

(57) Al-Sharif, A.; Jamal, M.; Zhang, L. X.; Larson, K.; Schmidt, T. a.; Jay, G. D.; Elsaid, K. a. *Arthritis Rheumatol.* **2015**, *67*, 1503–1513.

(58) Lee, S.; Müller, M.; Ratoi-Salagean, M.; Vörös, J.; Pasche, S.; Paul, S. M. De; Spikes, H. A.; Textor, M.; Spencer, N. D. *Tribol. Lett.* **2003**, *15*, 231–239.

(59) Perrino, C.; Lee, S.; Choi, S. W.; Maruyama, A.; Spencer, N. D. *Langmuir* **2008**, *24*, 8850–8856.

(60) Lee, S.; Shon, Y. S.; Colorado, R.; Guenard, R. L.; Lee, T. R.; Perry, S. S. *Langmuir* **2000**, *16*, 2220–2224.

(61) Wathier, M.; Lakin, B. a; Bansal, P. N.; Stoddart, S. S.; Snyder, B. D.; Grinstaff, M. W. *J. Am. Chem. Soc.* **2013**, 36–39.

(62) Singh, A.; Corvelli, M.; Unterman, S. A.; Wepasnick, K. A.; Mcdonnell, P.; Elissee, J. H. *Nat. Mater.* **2014**, *13*, 1–8.

(63) Schmidt, T. a; Gastelum, N. S.; Nguyen, Q. T.; Schumacher, B. L.; Sah, R. L. *Arthritis Rheum.* **2007**, *56*, 882–891.

(64) Swann, D. a; Silver, F. H.; Slayter, H. S.; Stafford, W.; Shore, E. *Biochem. J.* **1985**, *225*, 195–201.

(65) Banquy, X.; Burdyńska, J.; Lee, D. W.; Matyjaszewski, K.; Israelachvili, J. *J. Am. Chem. Soc.* **2014**, *136*, 6199–6202.

(66) Müller, M. T.; Yan, X.; Lee, S.; Perry, S. S.; Spencer, N. D. *Macromolecules* **2005**, *38*, 5706–5713.

(67) Müller, M.; Lee, S.; Spikes, H. A.; Spencer, N. D. *Tribol. Lett.* **2003**, *15*, 395–405.

(68) Jay, G. D.; Britt, D. E.; Cha, C. J. *J. Rheumatol.* **2000**, *27*, 594–600.

(69) Estrella, R. P.; Whitelock, J. M.; Packer, N. H.; Karlsson, N. G. *Biochem. J.* **2010**, *429*, 359–367.

(70) Pelet, J. M.; Putnam, D. *Macromolecules* **2009**, *42*, 1494–1499.

(71) Pelet, J. M.; Putnam, D. *Bioconjug. Chem.* **2011**, *22*, 329–337.

(72) Glinel, K.; Jonas, A. M.; Jouenne, T.; Leprince, J.; Galas, L.; Huck, W. T. S. *Bioconjug. Chem.* **2009**, *20*, 71–77.

(73) Bridges, A. W.; García, A. J. *J. diabetes Sci. Technol.* **2008**, *2*, 984–994.

(74) Bonnevie, E. D.; Puetzer, J. L.; Bonassar, L. J. *J. Biomech.* **2014**, *47*, 2183–2188.

(75) Gleghorn, J. P.; Bonassar, L. J. *J. Biomech.* **2008**, *41*, 1910–1918.

(76) Elsaid, K. a; Fleming, B. C.; Oksendahl, H. L.; Machan, J. T.; Fadale, P. D.; Hulstyn, M. J.; Shalvoy, R.; Jay, G. D. *Arthritis Rheum.* **2008**, *58*, 1707–1715.

(77) Elsaid, K. A.; Chichester, C.; Jay, G. D. In *Transactions of the Orthopedic Research Society*; 2001.

(78) Gleghorn, J. P.; Jones, a R. C.; Flannery, C. R.; Bonassar, L. J. *Eur. Cell. Mater.* **2007**, *14*, 20–28; discussion 28–29.

(79) Lahav, J.; Wijnen, E. M.; Hess, O.; Hamaia, S. W.; Griffiths, D.; Makris, M.; Knight, C. G.; Essex, D. W.; Farndale, R. W. *Blood* **2003**, *102*, 2085–2092.

(80) Flannery, C. R.; Yang, Z.; Zeng, W.; Sousa, E.; Li, N.; Liu, W.; Zollner, R.; He, T. *Trans. Orthop. Res. Soc.* **2010**, 20170.

(81) Jose De Souza, S.; Brentani, R. *J. Biol. Chem.* **1992**, *267*, 13763–13767.

(82) Rothenfluh, D. a; Bermudez, H.; O'Neil, C. P.; Hubbell, J. a. *Nat. Mater.* **2008**, *7*, 248–254.

(83) Kreikemeyer, B.; Talay, S. R.; Chhatwal, G. S. *Mol. Microbiol.* **1995**, *17*, 137–145.

(84) Talay, S. R.; Valentin-Weigand, P.; Jerlstrom, P. G.; Timmis, K. N.; Chhatwal, G. S. *Infect. Immun.* **1992**, *60*, 3837–3844.

(85) Peterlinz, K. a; Georgiadis, R. *Langmuir* **1996**, *12*, 4731–4740.

(86) Dėdinaitė, A. *Soft Matter* **2012**, *8*, 273.

(87) Kotlarz, H.; Gunnarsson, C. L.; Fang, H.; Rizzo, J. a. *Arthritis Rheum.* **2009**, *60*, 3546–3553.

(88) Das, S.; Banquy, X.; Zappone, B.; Greene, G. W.; Jay, G. D.; Israelachvili, J. N. *Biomacromolecules* **2013**, *14*, 1669–1677.

(89) Elsaid, K. a; Zhang, L.; Waller, K.; Tofte, J.; Teeple, E.; Fleming, B. C.; Jay, G. D. *Osteoarthritis Cartilage* **2012**, *20*, 940–948.

(90) Jay, G. D. *Curr. Opin. Orthop.* **2004**, *15*, 355–359.

(91) Zappone, B.; Ruths, M.; Greene, G. W.; Jay, G. D.; Israelachvili, J. N. *Biophys. J.* **2007**, *92*, 1693–1708.

(92) Chang, L. **2009**, 227–240.

(93) Dulin, J.; Drost, W. *Am. J. Vet. Res.* **2012**, *73*, 418–425.

(94) Lee, D. W.; Banquy, X.; Israelachvili, J. N. *Proc. Natl. Acad. Sci. U. S. A.* **2013**, *110*, E567–E574.

(95) Pritzker, K. P. H.; Gay, S.; Jimenez, S. a; Ostergaard, K.; Pelletier, J.-P.; Revell, P. a; Salter, D.; van den Berg, W. B. *Osteoarthritis Cartilage* **2006**, *14*, 13–29.

(96) Waller, K. a; Zhang, L. X.; Elsaid, K. a; Fleming, B. C.; Warman, M. L.; Jay, G. D. *Proc. Natl. Acad. Sci. U. S. A.* **2013**, *110*, 5852–5857.

(97) Elsaid, K. a; Machan, J. T.; Waller, K.; Fleming, B. C.; Jay, G. D. *Arthritis Rheum.* **2009**, *60*, 2997–3006.

(98) Kawano, T.; Miura, H.; Mawatari, T.; Moro-Oka, T.; Nakanishi, Y.; Higaki, H.; Iwamoto, Y. *Arthritis Rheum.* **2003**, *48*, 1923–1929.

(99) Swann, D. a.; Hendren, R. B.; Radin, E. L.; Sotman, S. L.; Duda, E. a. *Arthritis Rheum.* **1981**, *24*, 22–30.

(100) Teeple, E. *Am. J. Sports Med.* **2011**, *39*, 164.

(101) Billingham, J.; Breen, C.; Yarwood, J. **1997**, 19–34.

(102) Silverberg, J. L.; Barrett, A. R.; Das, M.; Petersen, P. B.; Bonassar, L. J. *Biophysj* **2014**, *107*, 1721–1730.

(103) Roberts, J. J.; Elder, R. M.; Neumann, A. J.; Jayaraman, A.; Bryant, S. J. *Biomacromolecules* **2014**, *15*, 1132–1141.

(104) Bures, P.; Huang, Y.; Oral, E.; Peppas, N. a. *J. Control. Release* **2001**, *72*, 25–33.

(105) Harris, J. M.; Chess, R. B. *Nat. Rev. Drug Discov.* **2003**, *2*, 214–221.